



HAL
open science

Neuronal Blockade of Thyroid Hormone Signaling Increases Sensitivity to Diet-Induced Obesity in Adult Male Mice

Eva Rial-Pensado, Laurence Canaple, Romain Guyot, Christoffer Clemmensen, Joëlle Wiersema, Shijia Wu, Sabine Richard, Anita Boelen, Timo Müller, Miguel López, et al.

► **To cite this version:**

Eva Rial-Pensado, Laurence Canaple, Romain Guyot, Christoffer Clemmensen, Joëlle Wiersema, et al.. Neuronal Blockade of Thyroid Hormone Signaling Increases Sensitivity to Diet-Induced Obesity in Adult Male Mice. *Endocrinology*, 2023, 164 (4), pp.bqad034. 10.1210/endo/bqad034 . hal-04041371

HAL Id: hal-04041371

<https://hal.science/hal-04041371v1>

Submitted on 22 Mar 2023

HAL is a multi-disciplinary open access archive for the deposit and dissemination of scientific research documents, whether they are published or not. The documents may come from teaching and research institutions in France or abroad, or from public or private research centers.

L'archive ouverte pluridisciplinaire **HAL**, est destinée au dépôt et à la diffusion de documents scientifiques de niveau recherche, publiés ou non, émanant des établissements d'enseignement et de recherche français ou étrangers, des laboratoires publics ou privés.

1 Neuronal blockade of thyroid hormone signaling increases sensitivity to diet-induced obesity in adult
2 male mice

3

4 Eva Rial Pensado^a, Laurence Canaple^{b,c}, Romain Guyot^b, Christoffer Clemmensen^{d,e}, Joëlle Wiersema^f,
5 Shijia Wu^b, Sabine Richard^b, Anita Boelen^f, Timo D. Müller^{d,g}, Miguel López^a, Frédéric Flamant^b, Karine
6 Gauthier^{b*}

7 ^a: NeurObesity Group, Department of Physiology, CiMUS, University of Santiago de Compostela,
8 Instituto de Investigación. Sanitaria & CIBER de la Fisiología de la Obesidad y la Nutrición (CIBEROBN),
9 Santiago de Compostela, Spain

10 ^b: Univ Lyon, ENS de Lyon, INRAE, CNRS, Institut de Génomique Fonctionnelle de Lyon, 69364 Lyon,
11 France

12 ^c: Univ Lyon, ENS de Lyon, Inserm US8, CNRS UMS3444, SFR Biosciences, 50 Avenue Tony Garnier, F-
13 69007 Lyon, France

14 ^d: Institute for Diabetes and Obesity, Helmholtz Diabetes Center at Helmholtz Zentrum München,
15 German Research Center for Environmental Health, Neuherberg, Germany

16 ^e: Novo Nordisk Foundation Center for Basic Metabolic Research, Faculty of Health and Medical
17 Sciences, University of Copenhagen, Copenhagen, Denmark

18 ^f: Endocrine Laboratory, Department of Clinical Chemistry, Amsterdam Gastroenterology &
19 Metabolism, Amsterdam UMC, University of Amsterdam, Amsterdam, The Netherlands.

20 ^g: German Center for Diabetes Research (DZD), Neuherberg, Germany.

21 ^{c,e}: present addresses

22 *: corresponding author and lead contact

23 Short title: Thyroid hormone in neurons and energy balance

24

25 Corresponding author informations :

26 Karine Gauthier

27 Univ Lyon, ENS de Lyon, INRAE, CNRS, Institut de Génomique Fonctionnelle de Lyon, 32-34 Avenue

28 Tony Garnier, 69007 Lyon, France

29 e-mail: karine.gauthier@ens-lyon.fr

30 Phone: +33 4 26 73 13 31

31 ORCID # 0000-0003-2961-6119

32 Funding

33 This work was supported by grants from the French ANR (FF Thyromut2 program; ANR-15-CE14-
34 0011-01); from ANSES (Thyrogenox); from Ministerio de Ciencia e Innovación co-funded by the EU
35 FEDER Program (ML: PID2021-128145NB-I00) and 'la Caixa' Foundation (ID 100010434), under the
36 agreement LCF/PR/HR19/52160022. ER-P was recipient of a fellowship from MINECO (BES-2015-
37 072743). CC is supported by the Lundbeck Foundation (Fellowship R238-2016-2859) and the Novo
38 Nordisk Foundation (grant number NNF17OC0026114). TDM received funding from the German
39 Research Foundation (DFG TRR296, TRR152, SFB1123 and GRK 2816/1), the German Center for
40 Diabetes Research (DZD e.V.) and the European Research Council ERC-CoG Trusted no.101044445.

41

42 Disclosures:

43 Declarations of interest: none

44 Data Availability :

45 Original data generated and analyzed during this study are included in this published article or in the
46 data repository listed in the references (<https://doi.org/10.6084/m9.figshare.22047992>).

47

48 **ABSTRACT**

49

50 Thyroid hormone increases energy expenditure. Its action is mediated by TR, nuclear receptors
51 present in peripheral tissues and in the central nervous system, particularly in hypothalamic neurons.
52 Here, we address the importance of thyroid hormone signaling in neurons, in general for the
53 regulation of energy expenditure.

54 We generated mice devoid of functional TR in neurons using the Cre/LoxP system. In hypothalamus,
55 which is the center for metabolic regulation, mutations were present in 20 to 42% of the neurons.

56 Phenotyping was performed under physiological conditions that trigger adaptive thermogenesis: cold
57 and high fat diet (HFD) feeding. Mutant mice displayed impaired thermogenic potential in brown and
58 inguinal white adipose tissues and were more prone to diet-induced obesity. They showed a
59 decreased energy expenditure on chow diet, and gain more weight on HFD. This higher sensitivity to
60 obesity disappeared at thermoneutrality. Concomitantly, the AMPK pathway was activated in the
61 ventromedial Hypothalamus (VMH) of the mutants as compared to the controls. In agreement
62 sympathetic nervous system (SNS) output, visualized by tyrosine hydroxylase expression was lower in
63 the brown adipose tissue (BAT) of the mutants. In contrast, absence of TR signaling in the mutants
64 did not affect their ability to respond to cold exposure.

65 This study provides the first genetic evidence that thyroid hormone signaling exerts a significant
66 influence in neurons to stimulate energy expenditure in some physiological context of adaptive
67 thermogenesis. TR function in neurons to limit weight gain in response to HFD and this effect is
68 associated with a potentiation of SNS output.

69 **Keywords**

70 Thyroid hormone, adaptive thermogenesis, cold exposure, diet induced obesity, neurons, brown

71 adipose tissue, sympathetic nervous system (SNS)

72

73

74 **1. Introduction**

75 As obesity and associated metabolic disorders became pandemic [1], the metabolic activities of
76 thyroid hormone (3,3',5-triiodo-L-thyronine, or T3), the active metabolite of thyroxine (T4) gained
77 renewed interest. Indeed, in humans, hyperthyroidism often results in weight loss, whereas
78 hypothyroidism tends to favor weight gain. Most importantly, exogenous T3 increases energy
79 expenditure (EE) both in humans and rodents [2]. As a result, an excess of T3 induces weight loss
80 despite an increase in food intake [3].

81 T3 can increase EE either directly or indirectly. Its direct metabolic action takes place in BAT, white
82 adipose tissue (WAT), muscle and liver, where it stimulates the mitochondrial metabolism. In BAT,
83 T4 can be deiodinated to produce T3. This local production of T3 triggers the expression of UCP1, the
84 protein responsible for the uncoupling between oxidative phosphorylation and ATP production,
85 which has an important function in thermogenesis [4-5]. After hormonal stimulation, several
86 enzymes involved in lipid synthesis and calories production are also induced in BAT [6], and EE
87 increases in muscle [7-8]. T3 also triggers WAT browning, *i.e.* the conversion of some white
88 adipocytes into thermogenic adipocytes producing UCP1 [9].

89 In addition to its direct influence on peripheral tissues, T3 is also involved in the central control of
90 adaptive thermogenesis [10-11], a process that is activated to face two types of external stress: cold
91 exposure and excess of food intake [12]. Perception of cold exposure by skin receptors is sensed by
92 the hypothalamus and results in an increased activity of the sympathetic nervous system (SNS). The
93 subsequent stimulation of adrenergic synapses in adipose tissues triggers immediate BAT
94 thermogenesis, and late browning of WAT [13-14]. SNS stimulation leads to both UCP1- dependent
95 and UCP1-independent thermogenesis in BAT [15-16-17] and muscle [18]. How a high-fat diet (HFD)
96 provokes a thermogenic response is less documented. While the involvement of the SNS in this
97 response is well established, the contribution of BAT seems limited [19-20]. Importantly, stimulation

98 of BAT *via* the SNS results in increased expression of the *Dio2* gene and a concomitant increase in
99 type-2 deiodinase (D2) activity [21]. The resulting local conversion of T4 into T3 contributes to an
100 increased thermogenic activity. *Dio2* knock-out mice are more sensitive to cold [20] and more prone
101 to diet-induced obesity (DIO) [22].

102 Hypothalamic glial cells including astrocytes and tanycytes contain D2, which allows a local
103 conversion of T4 into T3 [23]. The fact that this local conversion is involved in adaptative
104 thermogenesis is supported by experiments that show that an intrahypothalamic excess of T3 is
105 sufficient to stimulate BAT activity [10]. As all cell types in the hypothalamus express the nuclear
106 receptors of T3, either TR α 1 encoded by the *Thra* gene, or TR β 1/2 encoded by *Thrb* [24], they all
107 have the capacity to respond to a local increase in T3. However, the link between the intra-
108 hypothalamic T3 concentration and the increase in sympathetic tone remains unclear. Elevation of
109 intra-hypothalamic T3 concentration is characterized by rapid activation of the AMPK-ER stress-JNK1
110 pathway in neurons [25-10]. Although their T3 response is not documented, neuronal populations
111 located in other areas of the brain, notably the brainstem, also participate in EE [26].

112 We address here the importance of T3 signaling in neurons for the regulation of EE under
113 thermogenic stresses. To this end, we used the Cre/loxP methodology to produce a mouse model in
114 which the T3 response is selectively eliminated from a significant fraction of neurons, notably in 20 to
115 42% of the neurons in the hypothalamus depending of the nucleus. We evaluated the ability of these
116 mice to face thermogenic stress. Mice were exposed either to an intense cold or fed for several
117 months with an HFD. Mutant mice display an intact thermogenic response after exposure to cold at
118 4°C, but were more prone to DIO. The decrease in SNS tone in mutants mimics what was observed
119 after virogenetic inhibition of TR signaling in the hypothalamus and mirrors the increase triggered by
120 ICV T3 administration [10-25]. Overall, our data show that endogenous T3 signaling exerts a
121 significant influence on neurons involved in the regulation of energy metabolism.

122

123 **2. Material and Methods**

124 2.1 Chemicals:

125 Tri-iodothyronine (T3) and thyroxine (T4) were from Sigma-Aldrich (l'Isle D'Abeau, France).

126 2.2 Mice lines:

127 Mutant mice were obtained by crosses in the C57BL6/J genetic background to introduce different
128 recombinant alleles. *Thra*^{AMI} allows the production of the TR α 1^{L400R} mutant, which has dominant-
129 negative properties, after Cre/loxP-mediated excision of a stop cassette [27]. Despite the persistence
130 of an intact *Thra* allele in *Cre3^{Tg/+}xThra^{AMI/+}* mice, the dominant negative action of TR α 1^{L400R}
131 eliminates the capacity of cells expressing *Thra* to respond to T3. *Thrb*^{lox} has 2 tandem-arranged loxP
132 sequences, allowing Cre-mediated excision of exon 3, which encodes the DNA binding domain of the
133 TR β 1/TR β 2 receptor, resulting in a frameshift and a loss of function [28]. *Cre3^{Tg}* [29] is a randomly
134 integrated transgene that drives the expression of the Cre recombinase expression in neurons of the
135 central nervous system, but also the peripheral nervous system. The fraction of neurons with active
136 Cre differs in the different areas and is markedly higher in hypothalamus as compared to other areas
137 of the brain [30]. Cre activity was not detected in astrocytes or non-neuronal cell types [29-30]. We
138 previously verified this specific neuronal expression using the rosa YFP reporter line [31].
139 Furthermore, in the present study, using the *ROSA tdTomato* reporter transgene [32], we verified the
140 absence of recombination activity outside the nervous system, except for a small fraction of
141 cardiomyocytes (Fig. S1) [33]. *Cre3^{Tg/+}x ROSAtdTomato* mice were also used to highlight with red
142 fluorescence the hypothalamic cells in which Cre-mediated recombination occurred and compare the
143 percentage of neurons that present Cre activity in the different part of the hypothalamus (Fig. S2
144 [33]). Mice with the *Cre3^{Tg/+}xThra^{AMI/+}Thrb^{lox/lox}* genotype are called Neuron TRKO (NTRKO).
145 *Thra^{AMI/+}Thrb^{lox/lox}* littermates were used as controls (CTRL).

146 All experiments were carried out in accordance with the European Community Council Directive of
147 September 22, 2010 (2010/63/EU) regarding the protection of animals used for experimental and
148 other scientific purposes. The research project was approved in the different institutions. In Lyon, it

149 was approved by a local animal care and use committee (C2EA015) and subsequently authorized by
150 the French Ministry of Research, in Santiago by the USC Ethics Committee (Project ID 15010/14/006)
151 and in München by the Animal Ethics Committee of the government of Upper Bavaria, Germany. A
152 total of 180 mice have been used for this study.

153 2.3 Animal procedures and preparation of tissue samples:

154 2.3.1 Housing

155 Mice were fed an *ad libitum* LASQC Rod16 R diet (Altromin, Germany) (16.9% proteins; 4.3% fat and
156 79,2% carbohydrates, hereafter called CHOW), housed 2 per cage when possible, or otherwise
157 mentioned at 23°, under a 7:30 am: 8:30 pm light/dark cycle. 3- to 5- month-old male mice were
158 used for experiments.

159 2.3.2 Cold exposure and thermography

160 The cold response was assessed in mice implanted with IPTT-300 transponders (Plexx BV, The
161 Netherlands) by exposing them to 4°C for 58 hours. Infrared thermography was performed at
162 different time points in awake and free running animals. To capture static dorsal thermographic
163 images, thermal videos of 2 min duration each were recorded using an infrared camera (FLiR
164 Systems, Inc.). Thermal images were analyzed using the FLiR Research IR program. Regions of interest
165 (ROI) were drawn so that each type of ROI was overlaid on all thermal images at once. This allowed
166 for identical sizing of each type of ROI across all mice. An ROI on the basis of the tail served as the
167 temperature control, while an ROI surrounding the interscapular region served to evaluate BAT
168 thermogenesis. The temperature difference between these two ROI was calculated and used as a
169 proxy of BAT activation. For each time point, four images per mouse were analyzed. Four mice per
170 genotype were included in the experiment.

171 When mentioned, the experiments were performed at thermoneutrality in thermoregulated
172 chambers.

173 2.3.3 Induction of hypo/hyperthyroidism

174 T3 deficiency in adult animals was induced as previously described with a diet containing PTU
175 (Propylthiouracil) (Harlan Teklad TD95125, Madison, WI) (25.3% protein, 10% fat, 64.8%
176 carbohydrates and 0,15% PTU) and followed or not by thyroid hormones (TH) (mix of T4 and T3) daily
177 injections [34] for five consecutive days. Mice ate between 3.75 and 5.25 mg/day of PTU (2.5 and 3.5
178 g of diet per day). Serum concentrations of FT3 and FT4 were measured as described in paragraph
179 2.6, and were around 1 pm/L for both FT3 and FT4 in all genotypes in the PTU treated groups and
180 respectively above 50pm/L and 100mg/L (the maximum concentrations detectable by the assay) in
181 all genotypes in the PTU/TH treated groups. As expected PTU leads to hypothyroidism whereas TH
182 injection leads to hyperthyroidism.

183 2.3.4 HFD feeding

184 The response to HFD (Research Diets, New Brunswick, USA, D12331) (16.4 % proteins; 58% fat and
185 25.5% carbohydrates) was evaluated after acute feeding periods (3.5 days) or prolonged feeding
186 periods (3 to 7 months).

187 2.3.5 Indirect calorimetry

188 A calorimetric system (LabMaster; TSE Systems; Bad Homburg, Germany) was used to assess EE and
189 locomotor activity. Animals were placed one per cage with controlled conditions of air and
190 temperature (24°C). Mice were in adaptation for a week before starting the measurements. After
191 calibrating the system with the reference gases (20.9% O₂, 0.05% CO₂ and 79.05% N₂), the metabolic
192 rate was measured for 48 hours as previously described [35]. EE, RQ (VCO₂/VO₂) and LA were
193 recorded every 30 min. Mice were injected subcutaneously with 1 mg / kg of norepinephrine
194 bitartrate salt monohydrate (Sigma, Germany) to analyse the response to norepinephrine (NE). The
195 O₂ consumption was then measured for another 120-160 min every 10 min.

196 2.3.6 Tissue sampling

197 At the end of the experiments, mice were anesthetized at 2pm (intraperitoneal injection of a mixture
198 of xylazine and ketamine) to collect blood from the inferior vena cava in heparin coated tubes.
199 Plasma was obtained after centrifugation at 3500 rpm for 15mn. Tissues were dissected and snapped
200 frozen in liquid nitrogen and stored at -80°C for later RNA preparation or fixed in zinc formal Fixx
201 (ThermoFisher Scientific, Waltham, MA, USA) for histology and immunohistochemistry.

202 For neuroanatomy experiments, the thorax was opened and each mouse was perfused with 4%
203 paraformaldehyde in 0.1M phosphate buffer at room temperature and brain processed as previously
204 described [30]

205 2.4 RNA extraction and expression analyses by relative RT-qPCR

206 Total RNA was prepared using the TRI Reagent (ThermoFisher Scientific) protocol followed by a
207 RNase free DNase treatment (Qiagen, Hilden, Germany). Concentration and purity were quantified
208 with a Nanodrop. 1µg of RNA was used for reverse transcription with M-MLV reverse transcriptase
209 (Promega, Madison, WI, USA).

210 For qPCR, Protocols were described before [36] Duplicates were run for each sample. The results
211 were analyzed according to the $\Delta\Delta Cq$ method [37]. *Hprt* was used as the reference gene, and the
212 control group was CHOW fed, HFD fed or PTU CTRL groups. The numbers of mice used for each
213 experiment are reported in each figure legend. All the primer sequences are listed in Table S1 [33].

214 More details on the procedure is provided in supplemental data file S11 [33].

215 2.5 Western blot

216 The proteins were extracted from the hypothalamus in lysis buffer (50mM Tris-HCl, 10 mM EGTA,
217 1mM EDTA, 16mM Triton X-100, 1 mM sodium orthovanadate, 50mM sodium fluoride, 10 mM
218 sodium pyrophosphate and 250 mM sucrose). Western blots were transferred to PVDF membranes
219 (PVDF; Millipore; Billerica, MA, USA) and probed with antibodies against pACC α (Ser79) (Cell
220 Signaling Cat# 3661; RRID: AB_330337; Danvers; MA, USA), pAMPK α (Thr172) (Cell Signaling Cat#

221 2535S; RRID: AB_331250) or β -actin (Sigma-Aldrich Cat# A5316; RRID: AB_476743; St. Louis, MO,
222 USA) as described [8-9]. Adequate secondary antibody: anti-mouse (Agilent Cat# P0260, RRID:
223 AB_2636929; Santa Clara, CA, USA) or anti-rabbit (Agilent Cat# P0450, RRID: AB_2630354) was
224 added. Signal of autoradiographic films was quantified by densitometry using ImageJ-1.33 software
225 (NIH; Bethesda, MD, USA). Values were expressed in relation to β -actin. Data are expressed as a
226 percentage of CTRL vehicle and NTRKO vehicle. Representative images for all proteins are shown
227 with all bands for each picture derived from the same gel, although they may be spliced for clarity
228 (represented by vertical black lines). pACC α and pAMPK α were assayed in the same membranes,
229 therefore, some of the β -actin bands are common in their representative panels; this has been
230 specified in the appropriate figure legend.

231 2.6 Plasma biochemistry

232 Plasma was assayed on a Cobas 6000 automats for free T3 and free T4 with the Cobas e601 module
233 (Roche, ECL analyzers),

234 2.7 D2 activity

235 Hypothalamic block or 50 mg BAT tissue was homogenized in lysis buffer (100 mM sodium
236 phosphate, 2mM EDTA, 50mM DTT). D2 activity was measured in fresh homogenates. D2 activity was
237 measured in duplicate using 50 μ l undiluted homogenate (50 – 100 μ g protein) that was incubated
238 for 3h (hypothalamus) or 2h (BAT) at 37°C in a final volume of 100 μ l in the presence of 0.25 M
239 sucrose, 1 mM PTU (to block D1 activity in the hypothalamus), 500 nM of T3 (to block D3 activity in
240 the hypothalamus), 1 nM T4, and approximately $1 \cdot 10^5$ cpm 125 I-T4 (in-house, single labeled tracer
241 according to [38] Wiersinga *et al* in Phosphate-EDTA buffer (PE buffer, 100mM sodium phosphate,
242 2nM EDTA, pH7.2). D2 activity was expressed as 125 I- fmol released per minute per gram of protein.
243 The assay is based on the protocol previously described by Werneck-de-Castro *et al*. [39].

244 2.8 Histology, immunohistochemistry

245 2.8.1 Adipose tissues

246 Fixed adipose tissues were embedded in paraffin. Tissue sections (4 μm for BAT; 8 μm inguinal WAT
247 (iWAT) were stained with hematoxylin and eosin (H&E). Rabbit poly-clonal antibodies directed
248 against UCP1 (Abcam Cat# ab10983, RRID: AB_2241462, Cambridge, UK) and Tyrosine Hydroxylase
249 (Abcam Cat# ab112, RRID: AB_297840) were diluted in PBS/2.5% goat serum for immuno-
250 histochemistry, (1:400 and 1:750 dilution respectively). Sections were deparaffinized and incubated
251 overnight at 4°C with a primary antibody. Sections were then incubated with an HRP-labeled anti-
252 rabbit (1:300) (Promega Cat# W4011, RRID: AB_430833) for 1h at room temperature. Peroxidase
253 activity was visualized with diaminobenzidine staining (DAB, D5905 Sigma-Aldrich) and
254 counterstained with hematoxylin. The images were acquired using an AxioObserver Zeiss microscope
255 at a 16x magnification. Data were collected and the average intensity of the DAB signal was
256 quantified after color deconvolution was performed to separate the relative contributions of
257 DAB and hematoxylin, using ImageJ software. Background correction was performed using a
258 negative control slide, in which the primary antibody was omitted. Three slides per animal were
259 processed.

260 2.8.2 Brain

261 For neuroanatomy experiments, immunohistochemistry was performed on free-floating brain sections
262 as previously described [30]. Brain Coronal sections (50 μm) were cut with a vibrating microtome
263 (Integraslice 7550 SPDS, Campden Instruments, Loughborough, UK), and stored at -20°C in
264 cryoprotectant (30% ethylene glycol and 20% glycerol in 10 mM PBS) prior to immunohistochemistry.
265 The following primary antibodies were used: mouse anti-NeuN (1:500) (Merck Millipore Cat#
266 MAB377, RRID: AB_2298772, Burlington, MA, USA), and rabbit anti-GFAP (1:2000) (Agilent Cat#
267 Z0334, RRID: AB_10013382). Secondary antibodies were made in donkey (ThermoFisher Scientific,
268 anti-rabbit DyLight 488 Cat# SA5_10038, RRID: AB_2556618, anti-mouse DyLight 650 Cat#
269 SA5_10169, RRID:AB_25556749) and used at a 1:1000 dilution. Sections were imaged using an

270 inverted confocal microscope (Zeiss LSM 780). ImageJ software was used to estimate the proportion
271 of NeuN+ cells that were also tdTomato+ at different levels of the rostrocaudal hypothalamus.

272 *2.9 Quantification and statistical analyzes*

273 For mouse experiments, the data presented represent the average values of different animals from
274 the same genotype given the same treatment. The number of animals (n) used is indicated in the
275 figure legends. For RT-qPCR, each sample was run in duplicate. The error bars represent SEM, since it
276 is more appropriate than SD when $n \geq 6$. Statistical relevance was determined using the one-way
277 Anova or the T-Test method as indicated in the figure legends. * or \$ or £ stands for $p \leq 0,05$, ** or \$\$
278 for $0,005 \leq p \leq 0,05$, *** or \$\$\$ for $0,0005 \leq p \leq 0,005$, **** or \$\$\$\$ for $p \leq 0,0005$. This method is
279 appropriate since the size of the compared groups is similar and the distribution of the samples
280 normal. Given the variability of the phenotype that we observed, we used $n \geq 6$ to obtained
281 statistically significant results. For only two groups, $n = 5$, because the animals died during the
282 experimentation procedures. ns stands for non-significant.

283

284 **3.Results**

285 *3.1 Generation of mice with selective elimination of T3 signaling in neurons*

286 Recombination with the *Cre / LoxP* system was used to generate somatic mutations in the *Thra* and
287 *Thrb* genes. The *Cre3^{Tg}*, *Thra^{AMI}* and *Thrb^{lox}* alleles were combined to obtain *Cre3^{Tg/+}Thra^{AMI/+}Thrb^{lox/lox}*
288 mice, called NTRKO mice (see methods 2.2). These mice are heterozygous for the *Thra^{AMI}* mutation
289 and express the TR α 1^{L400R} in neurons as a result of Cre/loxP mediated recombination. This mutant
290 receptor exerts a dominant-negative activity toward the remaining intact TR α 1 receptor. As mice are
291 also homozygous for a *Thrb* floxed allele, *Cre/loxP* recombination eliminates the receptors encoded
292 by *Thrb* [27-28]. Therefore, the T3 response is selectively eliminated from all Cre expressing cells.

293 The efficacy of Cre-dependent recombination in the *Cre3^{Tg}* transgenic mice was first described to be
294 pan-neuronal in both the central and peripheral nervous systems [29]. Later studies from our lab
295 showed that the efficiency of recombination was the highest in hypothalamus as compared to other
296 brain area [30]. Here we used a Rosa-tdTomato^{lox} reporter [32] to show that Cre activity is merely
297 absent in non-nervous tissues (Fig. S1 [33]) and to better evaluate the recombination pattern in the
298 hypothalamus (Fig. S2 [33], Fig. 1). The red fluorescence systematically colocalized with the neuronal
299 NeuN marker and did not overlap with the glial marker GFAP (Fig. 1) as previously described in other
300 area of the brain [30]. The density of red fluorescent neurons was high in all hypothalamic nuclei (Fig.
301 1B, Fig. S2[33]), except the suprachiasmatic nucleus (not shown), representing 20 to 42% of all
302 neurons in the counted area (Fig. S2 [33]). Therefore, mutations take place in a large fraction of
303 neurons but not in glial cells or other cell types of the brain. We also used TRβ1 mRNA level as a
304 marker for Cre-mediated recombination in NTRKO mice and found that it was only decreased in the
305 hypothalamus but not in the peripheral tissues (Fig. 2A). As TRH is produced by the hypothalamic
306 neurons and involved in the feed-back control of TH production by the hypothalamus-pituitary axis,
307 we measured the expression of *TRH*. In NTRKO *TRH* levels were unchanged under either CHOW or
308 HFD (Fig. 2B left panel) and repression of *TRH* by TH in hypothyroid animals was also normal (Fig. 2B
309 right panel). In agreement free T3 and free T4 concentrations in serum were normal in the mutants
310 under all physiological conditions tested in the paper (Fig. S3A [33]).

311 In order to address the capacity of neurons to respond to T3, we treated NTRKO with PTU to make
312 them hypothyroid. In response to TH the expression of the *Shh* and *Klf9* genes, previously described
313 to be targets of T3 in neurons [36-40] was blunted in the hypothalamus of the mutants (Fig. 2C).
314 Moreover, whereas administration of TH increased food intake in CTRL mice [41], this response was
315 reduced in the NTRKO mice (Fig. 2D), supporting an inactivation of TH signaling in hypothalamic
316 neurons. In contrast, a normal TH response was observed in all peripheral tissues that we tested.
317 This was ascertained by measuring the mRNA levels for *Klf9* and *Hr* in inguinal WAT (iWAT), BAT and
318 heart, or *Hr* and *Thrsp* in liver (Fig. S3B [33]).

319 In summary, NTRKO mice are euthyroid with functional T3 signaling in all cell types except for a
320 fraction of neurons.

321

322 *3.2 T3 signaling in neurons regulates EE*

323 The NTRKO phenotype was first analyzed under standard conditions of food and temperature. Their
324 body weight (Fig. 3A) and temperature (Fig. 3B) were normal. Their EE (Fig. 3C) measured by indirect
325 calorimetry was lower than that of CTRL mice. Their locomotor activity (Fig. 3D) was similar but
326 NTRKO food intake (Fig. 3E) was slightly lower. RT-qPCR analyzes did not reveal any major alteration
327 of neither the thermogenic program in BAT (*Dio2*, *Ucp1*, *mCKB* and *mAlpl* mRNA) (Fig. S4A [33]) nor
328 the browning program in iWAT (*Ppargc1a*, *Ucp1*, *Cidea*, *Cox7c* and *Prdm6*) (Fig. S4B [33]). However,
329 UCP1 protein level was lower in BAT of NTRKO mice (Fig. 3F). We also assessed UCP1-independent
330 non-shivering thermogenesis in skeletal muscle, by measuring the expression of the genes involved
331 in Ca²⁺ cycling (*Serca2A*, *Serca2B*, *Sln*, *Ryr1*, *Ryr2*) [18]. We found an increase in *Ryr2* expression in
332 NTRKO muscles (Fig. 3G). Thermogenic mechanisms might be turned on in muscle to compensate
333 defective BAT activity.

334 *3.3 T3 signaling in neurons is not involved in severe cold-induced thermogenesis*

335 As increased D2 activity and local production of T3 in the BAT are critical to the cold response in wild-
336 type mice (WT) [21], the activity of D2 was checked in the hypothalamus of WT mice. It was not
337 modified during cold exposure in the hypothalamus but, as expected, was strongly induced in the
338 BAT (Fig. 4A).

339 To test whether despite the unchanged D2 activity in hypothalamus, impaired T3 signaling in neurons
340 prevents the cold-induced process of adaptive thermogenesis, mice were exposed to 4°C. Their body
341 weight (Fig 4B) and body temperature (Fig. 4C) were monitored for 2.5 days. Both NTRKO and CTRL
342 mice managed to maintain their body temperature by increasing their food intake (Fig. 4D).

343 Thermogenesis of BAT was observed by infrared thermography after 24 hours and 48 hours at 4°C.

344 The temperature of this tissue was similar in the two genotypes at both time points (Fig. S5A [33]).
345 Accordingly, the UCP1 protein was expressed at the same level in NTRKO and CTRL in both BAT (Fig.
346 4E) and in iWAT (Fig. S5B [33]) at 4°C. Moreover RT-qPCR analyzes did not reveal any major alteration
347 of either the thermogenic program in BAT (*Dio2*, *Ucp1*, *mCKB* and *mAlpl* mRNA) (Fig. 4E) or the
348 browning program in iWAT (*Ppargc1a*, *Ucp1*, *Cidea*, *Cox7c* and *Prdm6*) at this temperature (Fig. S5B
349 [33]).

350 The general response of BAT tissue to SNS stimulation, estimated by the level of expression of *Dio2*,
351 *Ucp1*, and *Elovl6*, is similar in the NTRKO BAT at 4°C compared to CTRL (Fig. 4F). However, the
352 expression of the *Adrb3* gene encoding the adrenergic receptor beta 3 the main sensor in BAT for
353 cold-triggered SNS activation, and of one of the genes up-regulated after this activation (*Ppargc1a*)
354 were higher in the NTRKO BAT under the same condition. A possible interpretation of these results
355 would be that a slight increase in BAT sensitivity to SNS stimulation allows NTRKO mice to face a cold
356 challenge.

357 *3.4 Inhibition of T3 signaling in neurons alters the response to DIO*

358 When fed an HFD, NTRKO mice gained more weight than CTRL (Fig. 5A). This resulted from higher
359 body fat accumulation (Fig. 5B) without any significant changes in food intake (Fig. 5C) or locomotor
360 activity (Fig. 5D). Circulating levels of total cholesterol and triglycerides were regulated on HFD to a
361 similar extent in both genotypes (Fig. S3C [33]). In WT animals, D2 enzymatic activity in the
362 hypothalamus increased slightly but significantly after 3.5 days of HFD (Fig. 5E). To characterize the
363 altered response of mutant mice to DIO, we measured gene expression in the BAT of NTRKO and
364 CTRL mice after an HFD. The expression of genes involved in the thermogenic program or the
365 response to SNS stimulation and the level of UCP1 protein were not affected (Fig. S6A [33]). The gene
366 expression analysis in muscle did not provide an indication of a defect in non-shivering
367 thermogenesis in NTRKO mice (Fig. S6B [33]). By contrast, quantification of *Ucp1* mRNA and UCP1

368 protein (Fig. 5F) in iWAT showed that browning was less efficient in the mutants under HFD.
369 Therefore, an impairment in iWAT browning might explain the observed sensitivity to DIO (Fig. 5A).

370 *3.5 Neuronal T3 signaling modulates SNS signaling to regulate EE*

371 Inefficient browning of iWAT under HFD, increased expression of the *Adrb3* gene in BAT at 4°C, and
372 decreased levels of UCP1 protein in both BAT and iWAT under different conditions, all point to
373 possible inadequate SNS signaling in NTRKO mutants. We housed mice at 30°C, to address the
374 sensitivity of mutant mice to DIO in the absence of thermogenic SNS stimulation [42]. In this
375 condition, obesity was more pronounced in CTRL mice than at 23°C (Δ body weight after 12 weeks of
376 HFD, 9 g versus 5 g at 23°C). Most importantly, the difference between mutant and control mice
377 disappeared at 30°C (Fig. S7A [33]). The level of UCP1 protein in BAT was similar in both genotypes
378 under the CHOW diet (Fig. S7B [33]) in contrast to what was observed at 23°C. Normalization of the
379 NTRKO phenotype at thermoneutrality provides a strong argument suggesting that the sensitivity of
380 NTRKO to DIO at 23°C originates from a defect in the tone of the SNS. To address the alternative
381 possibility, which would be that mutant thermogenic organs are less sensitive to SNS stimulation, we
382 treated NTRKO and CTRL mice with NE to activate β adrenergic receptor in BAT and measured the
383 induced change in EE (Fig. 6A). Mutant and control mice responded equally well to this stimulation,
384 reinforcing our initial interpretation. This was further reinforced by performing tyrosine hydroxylase
385 (TH) immunostaining in BAT and iWAT, which allows us to indirectly assess the autonomic nervous
386 input and adrenergic signaling on both CHOW (Fig. 6B) and HFD (Fig. 6C) [43]. This revealed a slight
387 alteration in the capacity of NTRKO mice to produce catecholamines on HFD (Fig. 6C).

388 We then assessed more directly the capacity of the hypothalamus to respond to a local T3
389 stimulation by performing intracerebroventricular (ICV) injections of T3 (Fig. 6 D, E and F). This
390 treatment reduced AMPK and acetyl-coA carboxylase (ACC) phosphorylation levels in the
391 hypothalamus of CTRL mice, as previously described [9-10-44] (Fig. 6D). Notably, the steady-state
392 levels of pAMPK α and pACC α was higher in NTRKO VMH than in the VMH of CTRL mice (Fig. 6E) and

393 was not decreased after local T3 injection (Fig. 6F). This supports the inhibitory effect of T3 on AMPK
394 signaling and the requirement for functional TR in neuron to mediate this response.

395 **4. Discussion**

396 Data published in recent years provided distinct but complementary pieces of information on the
397 mechanisms by which exogenous T3 influences energy homeostasis [9-10-11-44-45]. ICV or intra
398 VMH injection of T3 for short term or up to 28 days increases SNS tone, BAT activity and EE [9-10-44].
399 Despite increased UCP1 expression in BAT and iWAT, systemic hyperthyroidism increases EE also *via*
400 the activation of thermogenic mechanisms in the muscle [46-8]. Our study provides strong genetic
401 support to previous hypotheses drawn from these experiments and sheds light on the importance of
402 endogenous T3 signaling in neurons in facing thermogenic stresses.

403 Here we generated NTRKO, a new mouse model in which Cre- mediated mutations of TR in neurons
404 induce a selective blockade of T3 signaling in these neurons. In a previous study, using the same Cre
405 ($Cre3^{Tg/+}Thra^{AM1/+}$) Richard et al [30]. described that the expression of *hairless (Hr)*, a T3 target gene,
406 was deregulated in hypothalamus but not in other cerebral areas such as the hippocampus, the
407 cortex and the cerebellum. The hypothalamus must be one of the brain areas that is the most
408 impacted by the mutations. Here we show that the decrease of *Thrb* expression was only observed in
409 the hypothalamus and not in peripheral tissues. This decrease was only partial, since *Thrb* is also
410 expressed in glia and only 20 to 42% of neurons express Cre. However, it was sufficient to observe a
411 significant decrease of *Shh* and *Klf9* expression, two well described T3 target genes, in response to
412 T3. Importantly, the circulating levels of TH in NTRKO mice are similar to CTRL in all physiological
413 conditions tested and so is the regulation of *TRH* expression by TH. This suggests that TR are still
414 functional in TRH-expressing neurons to repress *TRH* expression in response to TH and that
415 regulation of the hypothalamo-pituitary-thyroid axis by TH remains unaltered in NTRKO mice.
416 Altogether these mice are euthyroid with functional T3 signaling in all cell types except for a fraction
417 of neurons mainly in hypothalamus.

418 Selective blockade of T3 signaling in NTRKO neurons triggers a decrease in EE that mirrors the
419 increase of EE previously described after T3 injection in the hypothalamus. Our data suggest that EE
420 is altered in NTRKO as a result of decreased uncoupling of catabolism and ATP production in BAT.
421 Calcium futile cycling in myotubes might produce heat at 23°C to compensate for the BAT defect and
422 to maintain normal body temperature in NTRKO mice under this mild cold stress.

423 Importantly, our data show that endogenous T3 signaling in neurons is mainly relevant for an
424 adequate response to HFD, as NTRKO manage to maintain body temperature after a cold challenge.
425 D2 activity is increased in the hypothalamus in response to HFD but not cold. That suggests that the
426 local production of T3 in the hypothalamus does not change during cold exposure and that the
427 neuronal response to T3 is not recruited for cold-induced adaptive thermogenesis. In contrast local
428 production of T3 in the hypothalamus would increase under HFD and the inability of NTRKO to
429 properly detect intrahypothalamic production of T3 would be responsible for their higher sensitivity
430 to DIO.

431 Interaction with the SNS is involved in the NTRKO sensitivity to DIO, as it is normalized at
432 thermoneutrality. Modulation of the hypothalamic AMPK pathway plays an important role in the
433 central action of T3 on both BAT and liver metabolism [9-10-44]. Our data show that while central T3
434 decreases pAMPK α and pACC α protein levels, the absence of T3 signaling in neurons increases the
435 basal level of these two phosphoproteins and blunts their regulation by T3. The expected result is a
436 reduced SNS tone to BAT in NTRKO mice at 23°C on CHOW diet. Consequently, under these
437 conditions the level of UCP1 protein in BAT is reduced. The associated decreased in BAT activity
438 might be responsible for the decrease in EE and could be compensated by alternative thermogenic
439 mechanisms, which include the activation of the Ca²⁺ futile cycle in the skeletal muscle to maintain
440 body temperature of NTRKO at 23°C. In any case, these results confirm that T3-induced
441 thermogenesis in the brain mostly relies on stimulation of the BAT, while peripheral T3
442 administration also stimulates not only BAT [6] but also muscle thermogenesis [8-46].

443 Thus, T3 signaling in neurons is an important player in the regulation of EE. The interference with the
444 AMPK regulation for SNS activation, previously described after central administration of T3, appears
445 to be also relevant when a physiological thermogenic stress stimulates the hypothalamic production
446 of T3. Importantly NTRKO mice efficiently maintained their body temperature when exposed to an
447 intense cold, displaying normal BAT and WAT response, despite a suboptimal SNS tone. We propose
448 a model for the role played by T3 in neurons for the regulation of EE in response to cold and HFD in
449 Figure 7.

450 This contrasts with data obtained in a mouse model that ubiquitously expressed TR α 1^{R384C} another
451 dominant negative TR α 1 [47]. Unlike NTRKO, these mice are hypermetabolic and hypothermic, with
452 a theoretical defended temperature of 38°C [48]. In depth phenotyping led to the conclusions that
453 this phenotype is primarily due to a chronic vasodilatation, which increases heat dissipation. The
454 defect in vasoconstriction was found to reflect a reduced sensitivity of blood vessels to SNS
455 stimulation [49] that should not take place in NTRKO mice.

456

457 *Conclusions*

458 We show that T3 does control EE under physiological stresses *via* its action in neurons. Moreover,
459 although selective inhibition of T3 signaling in neurons leads to a less severe metabolic phenotype
460 than hypothyroidism, modulation of T3 concentration and signaling in neurons definitively
461 represents a significant fraction of metabolic regulation by T3. Targeting T3 to neurons in adult might
462 help fight obesity.

463

464 *Limitations to our study*

465 First, the Cre-induced mutations occur in juveniles and are not restricted to adult life. Therefore, we
466 cannot rule out that the post-natal maturation of neuronal circuits is altered in mutant mice even so
467 we did not observe any obvious behavioral abnormality. Similarly, while the hypothalamus is the area
468 of the brain that displays the highest percentage of Cre-mediated recombination and that is known

469 to control EE, the intervention of other brain areas in the determination of the metabolic phenotype
470 of NTRKO is possible. Finally, only male mice were included in the study. Since sex specificity can
471 occur in metabolic responses, similar experiments should be run on females.
472 Further analyzes using models with selective inhibition of T3 signaling in other metabolic tissues,
473 specific neuronal populations, and other brain cell types would clarify the mechanism by which T3
474 regulates energy balance.

475 **Acknowledgements**

476 We thank Andres del Valle who contributed with RT-qPCR analyzes; Nadine Aguilera, Marie Teixeira,
477 and the ANIRA-PBES facility for help in transgenesis and mouse breeding; Catherine Cerrutti and the
478 members of the Flamant Lab for fruitful discussions and Marja van Veen for her technical help.

479 **Source of funding**

480 This work was supported by grants from the French ANR (FF Thyromut2 program; ANR-15-CE14-
481 0011-01); from ANSES (Thyrogenox); from Ministerio de Ciencia e Innovación co-funded by the EU
482 FEDER Program (ML: PID2021-128145NB-I00) and 'la Caixa' Foundation (ID 100010434), under the
483 agreement LCF/PR/HR19/52160022. ER-P was recipient of a fellowship from MINECO (BES-2015-
484 072743). CC is supported by the Lundbeck Foundation (Fellowship R238-2016-2859) and the Novo
485 Nordisk Foundation (grant number NNF17OC0026114). TDM received funding from the German
486 Research Foundation (DFG TRR296, TRR152, SFB1123 and GRK 2816/1), the German Center for
487 Diabetes Research (DZD e.V.) and the European Research Council ERC-CoG Trusted no.101044445.
488

489 **Author contributions**

490 KG, FF and ML conceived the study. KG, ER-P, CC ran the *in vivo* experiments. TDM participated in
491 study design and interpretation of data. LC ran the thermography experiments, and performed the
492 histology/immune histology studies, SW performed some immune histology studies, JW and AB

493 measured D2 activity. ER-P, KG, RG and SR performed *in vitro* experiments. KG, FF and ML wrote the
494 paper. All authors helped analyze the data, reviewed and commented on the final manuscript.

495

496 **Declaration of competing interest**

497 We declare no competing interest.

498 **Figure titles and legends**

499 *Fig. 1: Neuron-specific Cre-mediated recombination in the hypothalamus in mice that carry the Cre3*
500 *transgene (Cre3^{Tg/+}/ RosatdTomato⁺ mice).*

501 All cells expressing *tdTomato* (cre-mediated recombination reporter) also expressed NeuN (neuronal
502 marker), while none of them expressed GFAP (glial cell marker). For each field, 4 images of confocal
503 fluorescence microscopy are shown: tdTomato, combination of tdTomato and GFAP, NeuN,
504 combination of tdTomato and NeuN. (A) In the rostral hypothalamus, about 20% of NeuN+ cells also
505 expressed tdTomato. (B) In images with higher magnification, which were taken in the dorsomedial
506 hypothalamus, arrows have been added to help verify that all tdTomato+ cells were also NeuN+.

507 *Fig. 2: Characterization of the NTRKO mice: a model of selective blockade of T3 signaling in neurons.*

508 The selective activity of Cre recombinase in the *Cre3^{Tg}* transgenic line was evaluated by
509 immunohistochemistry using the *Cre3^{Tg/+}/ RosatdTomato⁺* reporter line (Fig. 1, Fig. S1). Different
510 experiments were done to demonstrate neuronal blockade of T3 signaling in NTRKO mice. (A) *Thrb*
511 expression was analyzed by relative RT-qPCR in different tissues of 3- to 4-month-old NTRKO (black
512 n=6) and CTRL (white n=6) males fed a CHOW diet. (B) 6-month-old male mice CTRL or NTRKO fed a
513 CHOW (n=5 and n=7) or an HFD for 3 months (n=5 and n=7) (left panel), or 3- to 4-month old males
514 from NTRKO and CTRL rendered hypothyroid by propyl-thio-uracil (PTU) and treated (n=6 per
515 genotype) or not by T3/T4 (TH) (n=6 per genotype) (right panel) were sacrificed and hypothalami
516 sampled for RNA preparation. The white and black columns, respectively, represent CTRL and

517 NTRKO. Expression of *TRH* was measured by relative RT-qPCR in the hypothalamus. (C) Expression of
518 well characterized T3 target genes (*Klf9*, *Shh*) was also measured in the hypothalamus of the same
519 PTU/PTUTH treated animals by relative RT-qPCR. CTRL PTU, NTRKO PTU, CTRL PTUTH, and NTRKO
520 PTUTH are, respectively, represented by white, black, light gray, and dark gray bars. (D) 3- to 4-
521 month old CTRL (white bars n=10) and NTRKO (black bars n=9) male mice were on CHOW diet and
522 injected daily with T3/T4 (TH) for 5 days from D0. Food intake was measured every day. CTRL animals
523 CHOW fed (A, B left panel and D) or PTU fed (B right panel and C) were taken as the reference group.
524 Statistical ANOVA tests were used for pairwise comparisons of CTRL and NTRKO mice. Stars indicated
525 a significant difference between CTRL and mutants in a given condition, dollars a significant
526 difference in a given genotype between two conditions. ns stands for non-significant.

527 *Fig. 3: T3 signaling in neurons regulates EE*

528 The different metabolic parameters were determined in 4-month-old CTRL (n=12) and NTRKO (n=12)
529 male mice housed at 23°C on a CHOW diet. We measured (A) Body weight (B) body temperature (C)
530 EE measured by indirect calorimetry (D), locomotor activity and (E) daily food intake. The gray-
531 shaded areas represent night time. (F) Six-month-old male mice CTRL and NTRKO fed a CHOW diet
532 (n=5 and n=7) at 23°C were sacrificed to sample BAT, iWAT. UCP1 immunostaining was performed
533 on BAT and iWAT slices and quantified by image analysis. (G). The expression of genes involved in
534 non-shivering thermogenesis was measured in the skeletal muscle of the same mice for RT-qPCR. The
535 white and black columns, respectively, represent CTRL and NTRKO. Statistical T- tests were used for
536 pairwise comparisons of CTRL and NTRKO mice in (A, B, C and D), statistical ANOVA tests for pairwise
537 comparisons of CTRL and NTRKO mice. ns stands for non-significant.

538

539 *Fig. 4: Blocking T3 signaling in neurons does not affect cold-induced thermogenesis*

540 (A) D2 activity was assayed in hypothalamus (Hy) and BAT of 2-month-old C57bl6 males maintained
541 for 58h at 4°C (n=6) (grey bars) or 23°C (n=6) (white bars). Five 4-month-old CTRL (n=6) and NTRKO

542 (n=6) male mice were housed at 4°C for 58 h. White and black squares/columns respectively
543 represent CTRL and NTRKO. (B) Body weight, (C) temperature as measured by telemetry and (D) food
544 intake were measured during cold exposure. BAT was sampled after cold-exposure for histology and
545 RT-qPCR analyzes. (E) (left panel) UCP1 immunostaining was performed on BAT slices and quantified
546 by image analysis. Markers of β adrenergic response/BAT activity in the BAT were analyzed by
547 relative RT-qPCR (right panel). Statistical ANOVA tests were used for pairwise comparisons of two
548 temperature in a given organ in (A), of CTRL and NTRKO mice in (B, C, D, E). ns stands for non-
549 significant.

550

551 *Fig.5: Blocking T3 signaling in neurons prevents adequate response to Diet Induced Obesity (DIO)*

552 2- to 3- month-old CTRL (n=9) and NTRKO (n=9) male mice were fed a CHOW diet and then switched
553 to an HFD (time 0). Their body weight was measured once a week. (A) Body weight gain (Δ body
554 weight) was calculated between any time point and the day diet was switched to HFD. (B) Body fat
555 mass was evaluated by echoMRI at 3 time points. (C) Daily food intake was measured and locomotion
556 (D) was studied for 4 consecutive days on HFD. (E) D2 activity was measured in the BAT and
557 hypothalamus (Hy) of 2-month-old C57bl6 mice fed either a CHOW diet (n=5) or an HFD (n=6) for 3.5
558 days. Tissues were sampled from 6-month-old male mice either CTRL or NTRKO fed an HFD for 3
559 months (n=5 and n=7). (F) iWAT were used for histology or RNA preparation. UCP1 immunostaining
560 was performed on iWAT slices (left panel). The expression of markers of browning in iWAT (right
561 panel) were assessed by relative RT-qPCR. The white and black columns, respectively, represent CTRL
562 and NTRKO. CTRL animals were taken as the reference group. Statistical T- tests were used for
563 pairwise comparisons of CTRL and NTRKO mice in (A, B, C and D). Statistical ANOVA tests were used
564 for pairwise comparisons of two temperature in a given organ in (E), of CTRL and NTRKO mice in (F).
565 C, D, E). ns stands for non-significant.

566

567 Fig. 6: *Neuron T3 signaling interferes with SNS signaling to regulate EE*
568 4-month-old CTRL and NTRKO male mice were injected (6 per genotype) (squares) or not with
569 norepinephrine (NE) (n=6 per genotype) (circles) at the time marked by an arrow. (A) EE was
570 recorded by indirect calorimetry before and after injection Tyrosine Hydroxylase (TH) is expressed in
571 nerve endings and catalyzes the production of NE. TH immunostaining was performed and quantified
572 on BAT (left panels) and iWAT (right panels) isolated from (B) CHOW-fed (n=5 for CTRL and n=7 for
573 NTRKO) or (C) HFD-fed (n=9 of each genotype) CTRL or NTRKO 6-month-old male mice housed at
574 23°C. 4-month-old CTRL and NTRKO male mice were ICV injected with T3 (n=6 per genotype) or
575 vehicle (VEH) (n=6 per genotype). After dissection, proteins were extracted from VMH and the
576 quantity of pAMPK α and pACC α estimated by western blot. β -actin is used for normalization. (D/E/F)
577 Blots are provided on the left, (D/E/F) their quantification on the right. The previously described
578 effect of T3 in CTRL is depicted in (D), the effect of the mutation is in (E), and the lack of effect of T3
579 in NTRKO in (F). In the western blot analyses, values were expressed in relation to β -actin.
580 Representative images for all proteins are shown; all the bands for each picture are derived from the
581 same gel, although they may be spliced for clarity (represented by vertical black lines). pAMPK α and
582 pACC α were assayed in the same membranes, therefore, some of the β -actin bands are common in
583 their representative panels, this has been specified in Figures 6D-F. (A, D, E and F) Statistical T- tests
584 or (B,C) Statistical ANOVA tests were used for pairwise comparisons in (B, C, E) of CTRL and NTRKO
585 mice , in (A) of CTRL NE and CTRL (S) and of NTRKO NE and NTRKO , in (D) of CTRL T3 and CTRL VEH
586 and in (F) of NTRKO T3 and NTRKO VEH. ns stands for non-significant.

587 Fig. 7: *Proposed model for the role of T3 in neurone for regulation of energy expenditure in response*
588 *to cold and HFD*

589 On the left panel, a scheme of regulation of energy expenditure in response to cold and HFD in CTRL
590 mice. Black arrows picture the regulation observed under either COLD or HFD stimuli as compared
591 respectively to 23°C and CHOW diet (the amplitude of the response might be different under cold

592 and HFD). The Blue arrows the regulation observed only at 4°C, the red the regulation observed only
593 under HFD. The lightening sign stands for activation.
594 On the right panel are summarized three situation in the NTRKO. In green it shows, the difference of
595 energy regulation pathways in the NTRKO as compared to CTRL on regular conditions (CHOW and
596 23°C). Black arrows picture the regulation observed in NTRKO under either COLD or HFD as
597 compared respectively to 23°C and CHOW diet. Red arrows picture the regulation observed only
598 under HFD as compared to CHOW in the NTRKO and the Blue arrows the regulation only observed at
599 4°C as compared to 23°C in NTRKO as well.

600 **References:**

- 601 [1] Blüher, M., 2019. Obesity: global epidemiology and pathogenesis. *Nat Rev Endocrinol.*
602 *May;15(5):288-298*
- 603 [2] Zekri, Y., Flamant, F., Gauthier, K., 2021. Central vs. Peripheral Action of Thyroid Hormone in
604 Adaptive Thermogenesis: A burning topic. *Cells 10(6):1327*
- 605 [3] Cicatiello, A.G., Di Girolamo, D., Dentice, M., 2018. Metabolic Effects of Intracellular Regulation
606 of Thyroid Hormone: Old Players, New Concepts. *Front Endocrinol Sep. 11; 9:474*
- 607 [4] Chouchani, E.T., Kazak, L.L., Spiegelman, B.M., 2019. New Advances in Adaptive
608 Thermogenesis: UCP1 and Beyond. *Cell Metab. Jan. 8;29(1):27-37*
- 609 [5] Golozoubova, V., Cannon, B., Nedergaard, J., 2006. UCP1 is essential for adaptive adrenergic
610 nonshivering thermogenesis *Am. J. Physiol. Endocrinol. Metab. 291: E350-E357*
- 611 [6] Zekri, Y., Guyot, R., Suñer, I.G., Canaple, L., Stein, A.G., Petit, J.V., et al. 2022. Brown adipocytes
612 local response to thyroid hormone is required for adaptive thermogenesis in adult male mice.
613 *Elife. Nov 14;11:e81996.*
- 614 [7] Obregon, M.J., 2014. Adipose tissues and thyroid hormones. *Front Physiol. 5: 479.*

615 [8] Nicolaisen, T.S., Klein, A.B., Dmytriyeva, O., Lund, J., Ingerslev, L.R., Fritzen, A.M., et al. 2020.
616 Thyroid hormone receptor alpha in skeletal muscle is essential for T3-mediated increase in energy
617 expenditure. *FASEB J.* 34(11):15480-15491.

618 [9] Martinez-Sánchez, N., Moreno-Navarrete, J.M., Contreras, C., Rial-Pensado, E., Fernø, J.,
619 Nogueiras, R., et al. 2017. Thyroid hormones induce the browning of white fat. *J*
620 *Endocrinol* 232(2):351-362

621 [10] López, M., Varela, L., Vázquez, M.J., Rodríguez-Cuenca, S., González, C.R., Velagapudi, V.R., et
622 al. 2010. Hypothalamic AMPK and fatty acid metabolism mediate thyroid regulation of energy
623 balance. *Nat Med.* 16 (9):1001-8

624 [11] Capelli, V., Diéguez, C., Mittag, J., López, M., 2021. Thyroid wars : the rise of central actions.
625 *Trends Endocrinol Metab. Sep;32(9):659-671*

626 [12] Cannon, B., Nedergaard, J., 2004. Brown adipose tissue: Function and Physiological Significance.
627 *Physiol Rev. Jan; 84: 277-359*

628 [13] Fliers, E., Klieverik, L.P., Kalsbeek, A., 2010. Novel neural pathways for metabolic effects
629 of thyroid hormone. *Trends Endocrinol Metab. Apr;21(4):230-6*

630 [14] López, M., Alvarez, C.V., Nogueiras, R., Diéguez, C., 2013. Regulation of energy balance by
631 thyroid hormones at central level. *Trends Mol Med Jul;19(7):418-27*

632 [15] Kazak, L., Chouchani, E.T., Jedrychowski, M.P., Erickson, B.K., Shinoda, K., Cohen, P., et al. 2015.
633 A creatine-driven substrate cycle enhances energy expenditure and thermogenesis in beige fat. *Cell*
634 *22; 163(3):643-55*

635 [16] Rahbani, J.F., Roesler, A., Hussain, M.F., Samborska, B., Dykstra, C.B., Tsai, L., 2021. Creatine
636 kinase B controls futile creatine cycling in thermogenic fat. *Nature* 590 (7846):480-485.

637 [17] Sun, Y., Rahbani, J.F, Jedrychowski, M.P., Riley, C.L., Vidoni, S., Bogoslavski, D., et al. 2021.
638 Mitochondrial TNAP controls thermogenesis by hydrolysis of phosphocreatine. *Nature* 593
639 (7860):580-585.

640 [18] Bal, N.C., Maurya, SK., Periasamy, M., 2018. The Role of Sarcolipin in Muscle Nonshivering
641 Thermogenesis. *Front Physiol.* 9:1217

642 [19] Saito, M., Matsushita, M., Yoneshiro, T., Okamatsu-Ogura, Y., 2020. Brown adipose tissue, diet-
643 induced thermogenesis, and Thermogenic Food Ingredients: From Mice to Men. *Front Endocrinol*
644 11:222.

645 [20] L.P. Kozak, L.P., 2020. Brown fat and the myth of diet-induced thermogenesis. *Cell Metab*
646 11(4):263-7.

647 [21] de Jesus, L.A., Carvalho, S.D., Ribeiro, M.O., Schneider, M., Kim, S.W., Harney, J.W., *et al.* 2001.
648 The type 2 iodothyronine deiodinase is essential for adaptive thermogenesis in brown adipose tissue.
649 *J Clin Invest* 108(9):1379-85

650 [22] Castillo, M., Hall, J.A., Correa-Medina, M., Ueta, C., Kang, H.W., Cohen, D.E., et al. 2011.
651 Disruption of thyroid hormone activation in type 2 deiodinase knockout mice causes obesity with
652 glucose intolerance and liver steatosis only at thermoneutrality *Diabetes* 60(4):1082-9

653 [23] A. Guadaño-Ferraz, A., Obregón, M.J., St. Germain, D.L., Bernal, J., 1997. Type 2 iodothyronine
654 deiodinase is expressed primarily in glial cells in the neonatal rat brain. *PNAS* 94 (19) 10391-10396

655 [24] Samarut, J., Plateroti, M., 2018. Thyroid Hormone Receptors: Several players for
656 One Hormone and Multiple Functions. *Methods Mol Biol.* 1801:1-8

657 [25] Martínez-Sánchez, N., Seoane-Collazo, P., Contreras, C., Varela, L., Villarroya, J., Rial-Pensado, E.,
658 et al. 2017. Hypothalamic AMPK-ER Stress-JNK1 Axis Mediates the Central Actions of Thyroid
659 Hormones on Energy Balance. *Cell Metab.* 26(1):212-229

660 [26] Roh, E., Kim, M.S., 2016. Brain regulation of Energy Metabolism. *Endocrinol Metab* (Seoul).
661 31(4):519-524.

662 [27] Quignodon, L., Vincent, S., Winter, H., Samarut, J., Flamant, F., 2007. A point mutation in the 2
663 domain of thyroid hormone receptor alpha1 expressed after CRE-mediated recombination partially
664 recapitulates hypothyroidism. *Mol Endocrinol.* 21(10):2350-60

665 [28] Winter, H., Rüttiger, L., Müller, M., Kuhn, S., Brandt, N., Zimmermann, U., et al. 2009. Deafness
666 in TRbeta mutants is caused by malformation of the tectorial membrane. *J Neurosci.* 29(8):2581-7

667 [29] Banares, S., Zeh, K., Krajewska, M., Kermer, P., Baribault, H., Reed, J.C., et al. 2005. Novel pan
668 neuronal Cre transgenic line for conditional ablation of genes in the nervous system.
669 *Genesis* May;42(1):6-16

670 [30] Richard, S., Aguilera, N., Thévenet, M., Dkhissi-Benyahya, O., Flamant, F., 2017. Neuronal
671 expression of a thyroid hormone receptor α mutation alters mouse behavior. *Behav Brain Res Mar*
672 15; 321:18-27

673 [31] Srinivas, S., Watanabe, T., Lin, C.S., William, C.M., Tanabe, Y., Jessell, T.M., et al. 2001. Cre
674 reporter strains produced by the targeted insertion of EYFP and ECFP into the ROSA26 locus. *BMC*
675 *Dev. Biol.* 1; 4

676 [32] Madisen, L., Zwingman, T.A., Sunkin, S.M., Oh, S.W., Zariwala, H.A., Gu, H. et al. 2010. A robust
677 and high-throughput Cre reporting and characterization system for the whole mouse brain. *Nat*
678 *Neurosci.* Jan; 13(1): 133-40

679 [33] Rial Pensado, E., Canaple, L., Guyot, R., Clemmensen, C., Wiersema^f, J., Shijia Wu, S. ERP
680 Supplemental data file. Doi : 10.6084/m9.figshare.22047992

681 [34] Weiss, R.E., Murata, Y., Cua, K., Hayashi, Y., Seo, H., Refetoff, S., 1998. Thyroid hormone action
682 on liver, heart, and energy expenditure in thyroid hormone receptor beta-deficient mice.
683 *Endocrinology* 139, 4945-4952. Erratum in: *Endocrinology.* (2000) 141, 4767

684 [35] Imbernon, M., Beiroa, D., Vázquez, M.J., Morgan, D.A., Veyrat-Durebex, C., Porteiro, B., et al.
685 2013. Central melanin-concentrating hormone influences liver and adipose metabolism through
686 specific hypothalamic nuclei and efferent autonomic/JNK1 pathways. *Gastroenterology*
687 Mar;144(3):636-649

688 [36] Chatonnet, F., Guyot, R., Benoît, G., Flamant, F., 2013. Genome-wide analysis of thyroid
689 hormone receptors shared and specific functions in neural cells. *Proc Natl Acad Sci U S A* Feb
690 19;110(8): E766-75.

691 [37] Bookout, A.L., Mangelsdorf, D.J., 2003. Quantitative real-time PCR protocol for analysis of
692 nuclear receptor signaling pathways. *Nucl Recept Signal*. 1: e012

693 [38] Wiersinga, W.M., Chopra, I.J., 1982. Radioimmunoassay of thyroxine (T4), 3,5,3'-triiodothyronine
694 (T3), 3,3',5'-triiodothyronine (reverse T3, rT3) and 3,3'-diiodothyronine (T2). *Methods Enzymol*.
695 84:272-303

696 [39] Werneck-de-Castro, J.P., Fonseca, T.L., Ignacio, D.L., Fernandes, G.W., Andrade-Feraud, C.M.,
697 Lartey, L.J., et al. 2015. Thyroid hormone signaling in Male Mouse Skeletal Muscle Is Largely
698 Independent of D2 in myocytes. *Endocrinology*. Oct;156(10):3842-52

699 [40] Desouza, L.A., Sathanoori, M., Kapoor, R., Rajadhyaksha, N., Gonzalez, L.E., Kottmann, A.H., et al.
700 2011. Thyroid hormone regulates the expression of the sonic hedgehog signaling pathway in the
701 embryonic and adult Mammalian brain. *Endocrinology* 152(5):1989-2000.

702 [41] Kong, W.M., Martin, N.M., Smith, K.L., Gardiner, J.V., Connoley, I.P., Stephens, D.A., et al. 2004.
703 Triiodothyronine Stimulates Food Intake via the Hypothalamic Ventromedial Nucleus Independent of
704 Changes in Energy Expenditure. *Endocrinology* Vol 145; 11: 5252–5258

705 [42] Ganeshan, K., Chawla, A., 2017. Warming the mouse to model human diseases. *Nat Rev*
706 *Endocrinol*. Aug;13(8):458-465

707 [43] de Matteis, R., Ricquier, D., Cinti, S., 1998. Immunoreactive nerves of TH, NPY, SP, and CGRP in
708 interscapular brown adipose tissue of adult rats acclimated to different temperatures: an
709 immunohistochemical study. *J. Neurocytol* 27, 877–886

710 [44] Alvarez-Crespo, M., Csikasz, R.I., Martínez-Sánchez, N., Diéguez, C., Cannon, B., Nedergaard,
711 J., et al. 2016. Essential role of UCP1 in modulating the central effects of thyroid hormones on energy
712 balance. *Mol Metab.* 5(4):271-282

713 [45] Zhang, Z., Foppen, E., Su, Y., 2016. Metabolic effects of Chronic T₃ Administration in the
714 hypothalamic paraventricular and Ventromedial Nucleus in male rats. *Endocrinology*
715 *Oct*;157(10):4076-4085

716 [46] Johann, K., Cremer, A.L., Fischer, A.W., Heine, M., Pensado, E.R., Resch, J., et al. 2019. Thyroid
717 hormone-induced browning of white adipose tissue does not contribute to Thermogenesis and
718 Glucose Consumption. *Cell Rep.* 27(11):3385-3400

719 [47] Tinnikov, A., Nordström, K., Thorén, P., Kindblom, J.M., Malin, S., Rozell, B., et al. 2002.
720 Retardation of post-natal development caused by a negatively acting thyroid hormone
721 receptor alpha1. *EMBO J. Oct.* 1;21(19):5079-87

722 [48] Sjögren, M., Alkemade, A., Mittag, J., Nordström, K., Katz, A., Rozell, B., et al. 2007.
723 Hypermetabolism in mice caused by the central action of an unliganded thyroid hormone
724 receptor alpha1. *EMBO J. Oct* 31; 26(21): 4535–4545.

725 [49] Warner, A., Rahman, A., Solsjö, P., Gottschling, K., Davis, B., Vennström, B., et al. 2013.
726 Inappropriate heat dissipation ignites brown fat thermogenesis in mice with a mutant thyroid
727 hormone receptor α 1. *Proc Natl Acad Sci U S A. Oct* 1;110(40):16241-6

728
729
730
731

Fig. 1: color

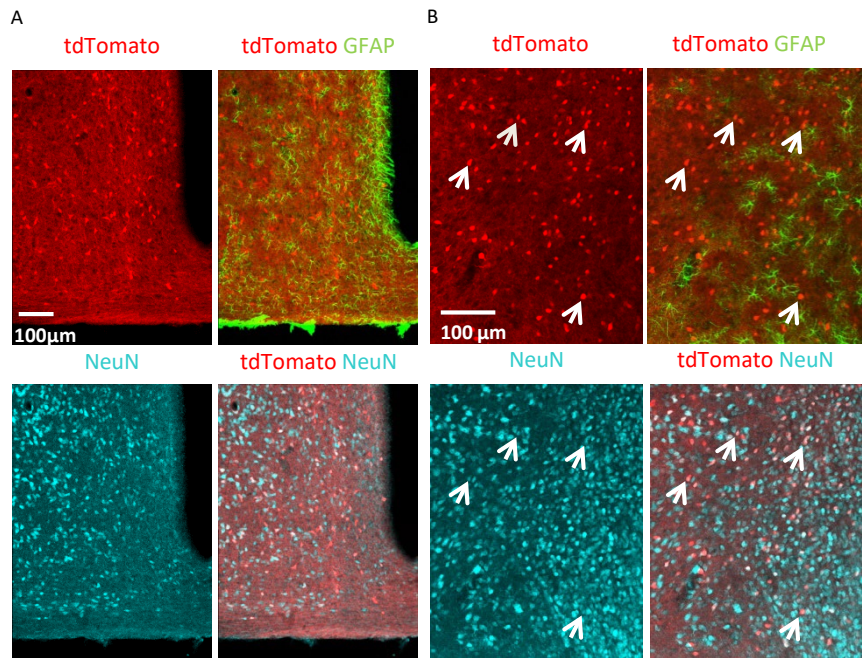


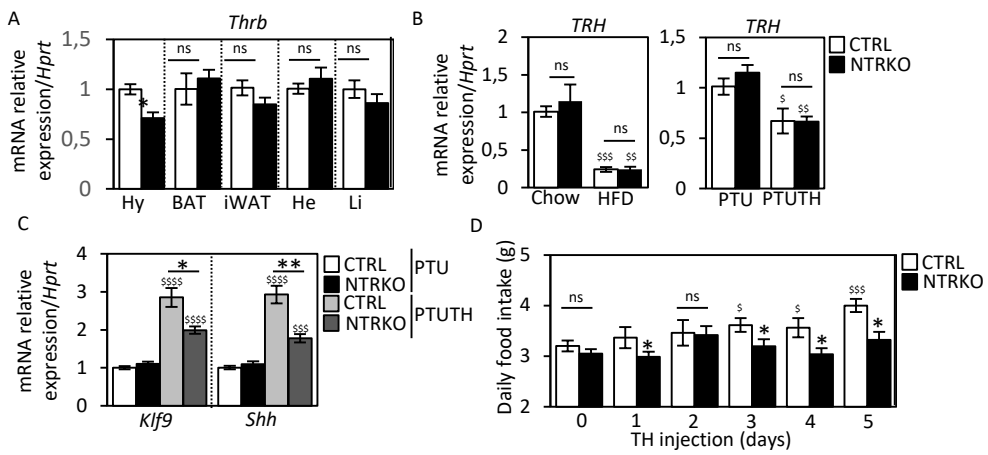
Fig. 2

Fig. 3: color

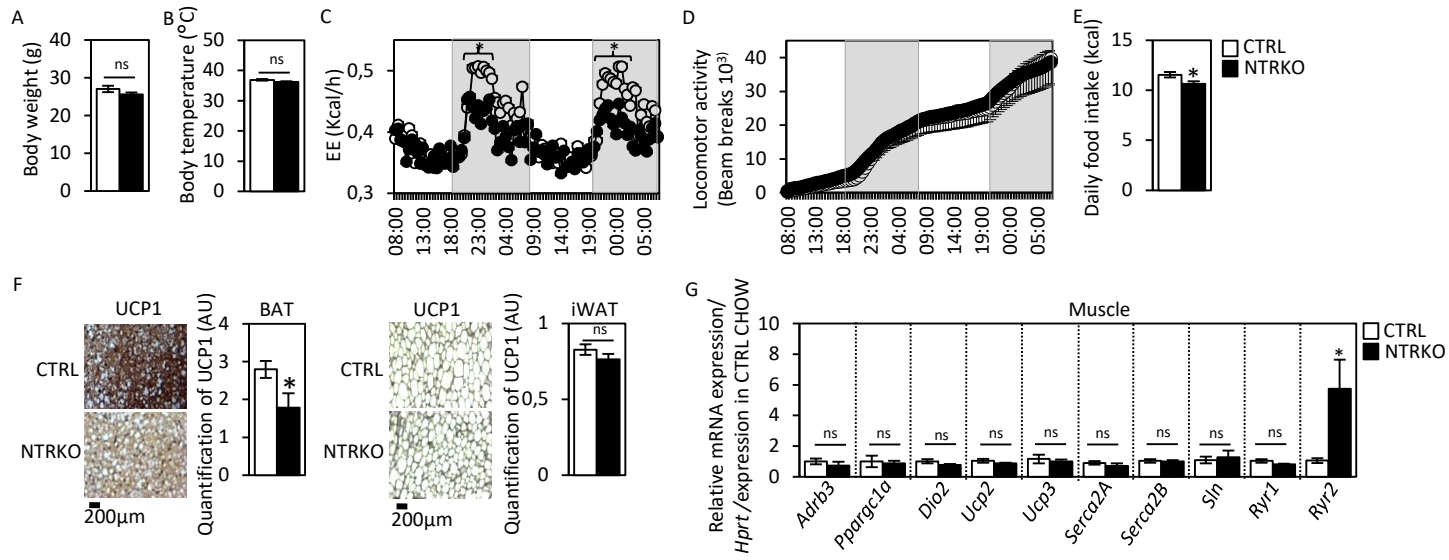


Fig. 4: color

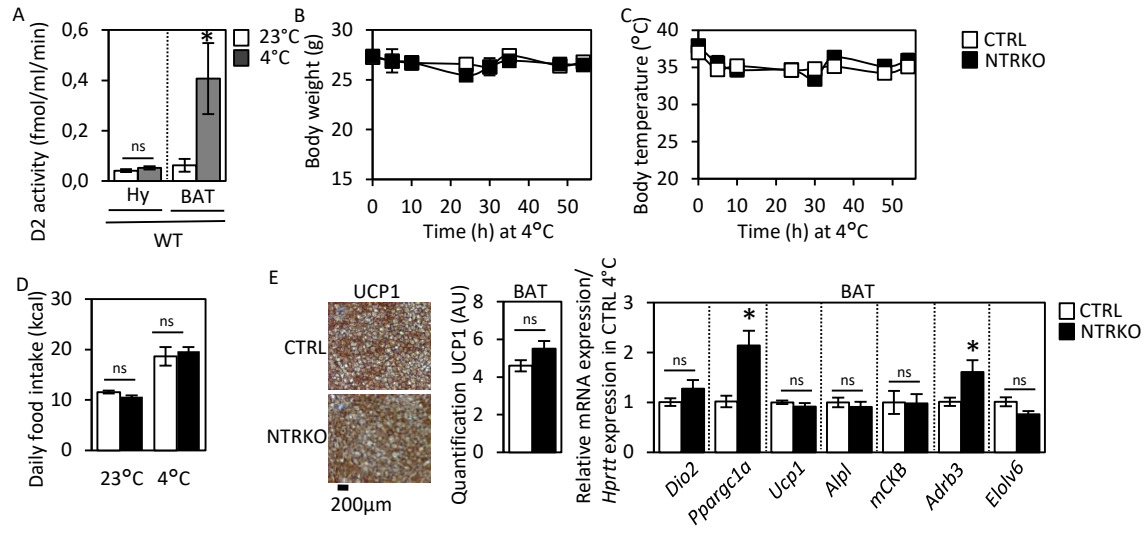


Fig. 5: color

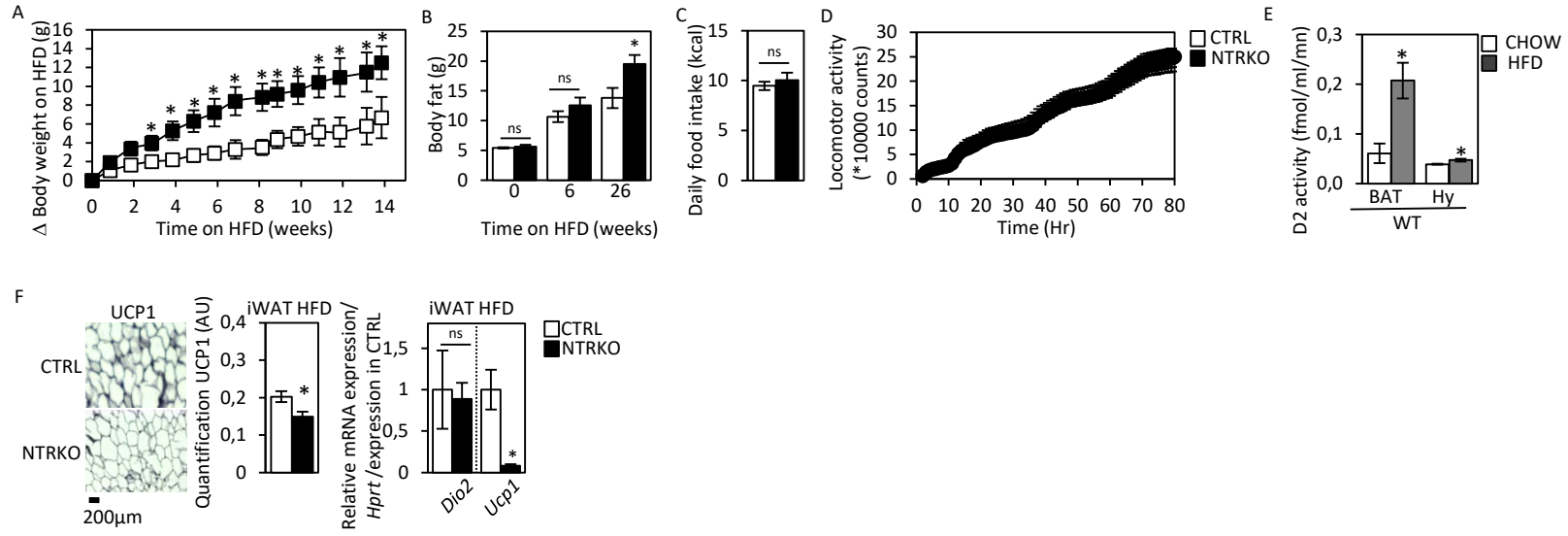
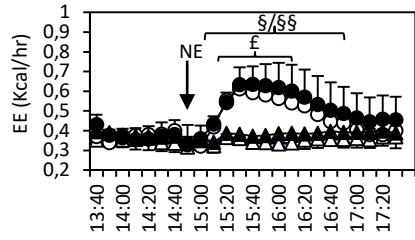
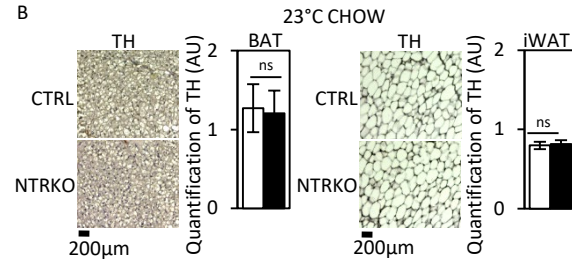


Fig. 6: color

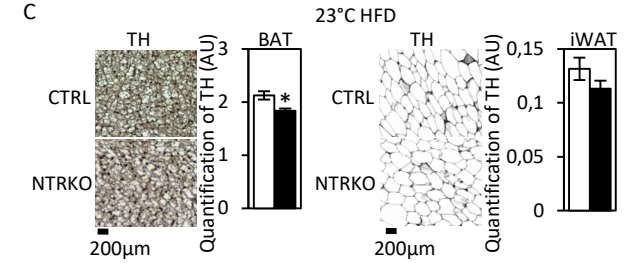
A



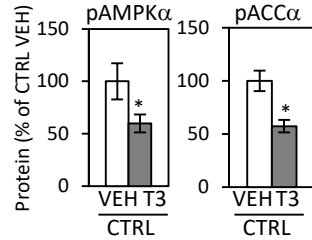
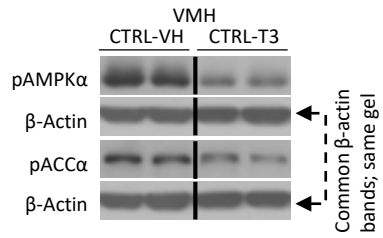
B



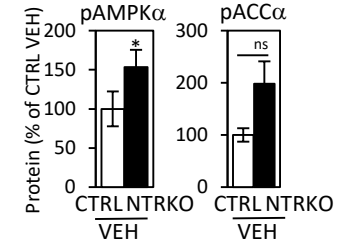
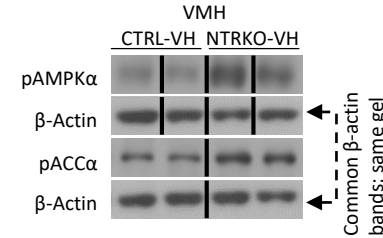
C



D



E



F

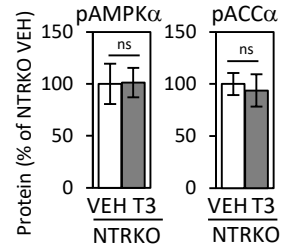
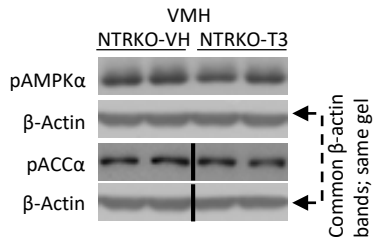
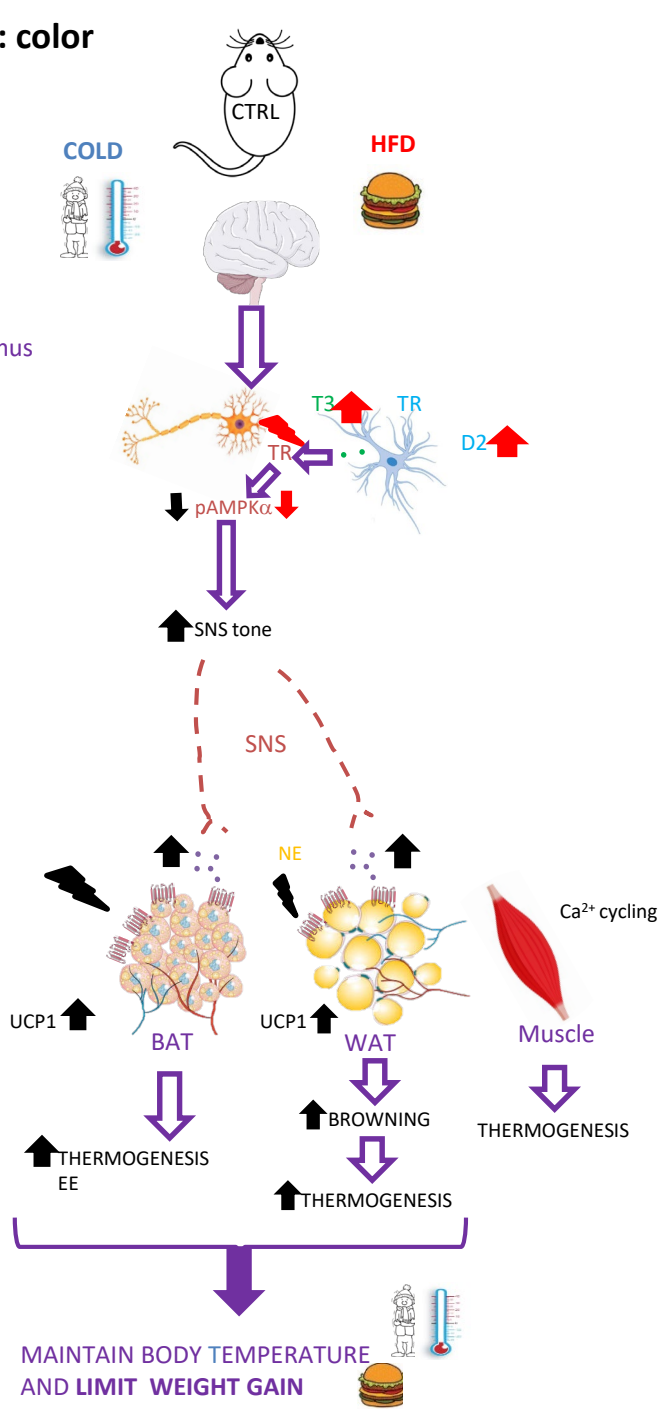
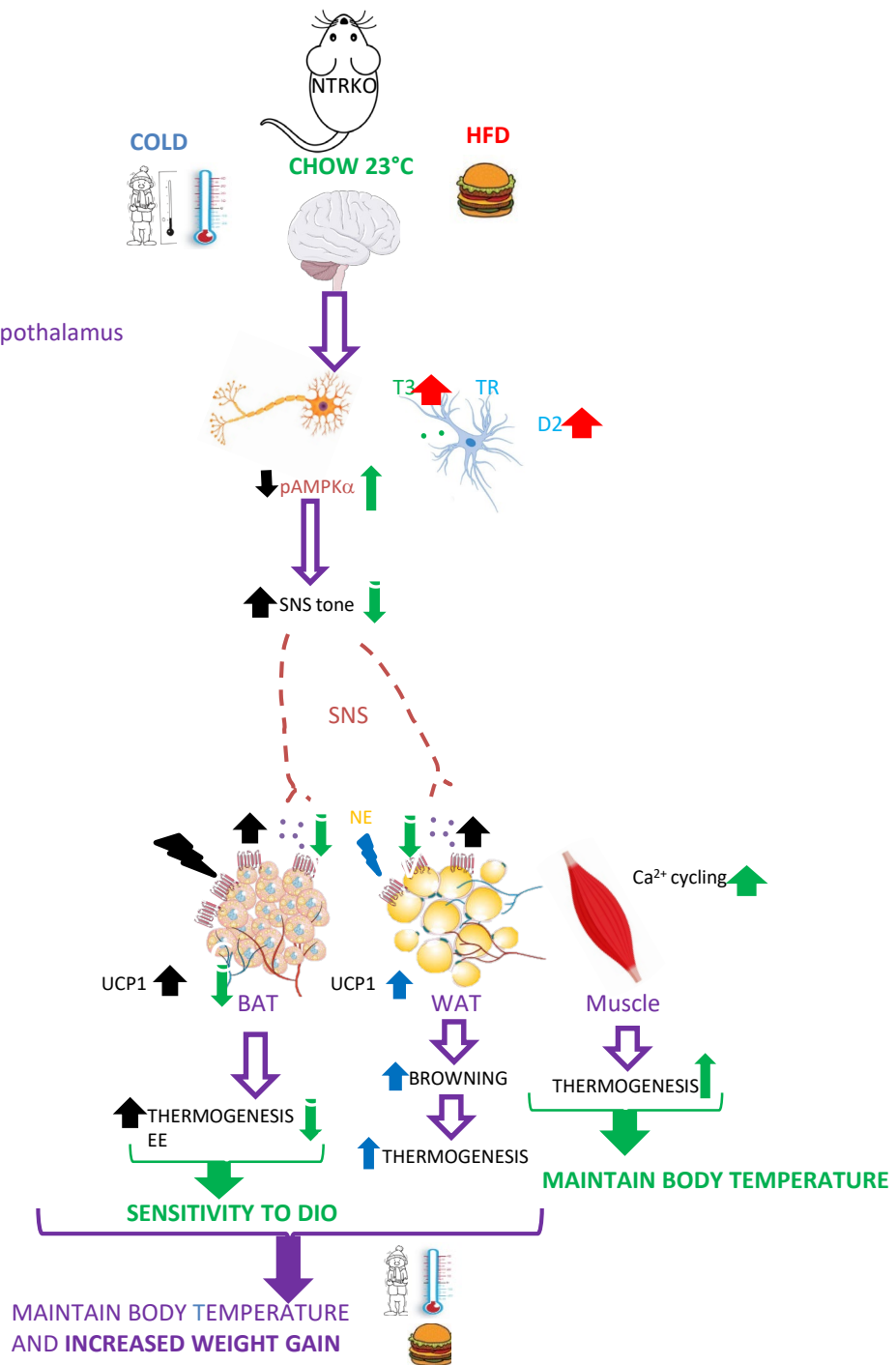


Fig. 7: color

Hypothalamus



Hypothalamus



Supplemental information

SI1

RNA extraction and expression analyzes by relative RT-qPCR: detailed procedure

RNA extraction

Total RNA was prepared using the TRI Reagent (ThermoFisher Scientific) protocol followed by a RNase free DNase treatment (Qiagen). Reaction was stopped by EDTA. Concentration and purity was quantified with a Nanodrop.

Reverse transcription:

- Heat 1 µg RNA in 9,5 µl H₂O + 1 µl Random Hexamer Primer 100ng/µl, 70°C 5 min. Put on ice after the 5mn to avoid re-hybridization of RNAs.
- Add 9,5µl of MIX (4µl 5X MLV buffer Promega, 2 µl dNTP (5mM each), 0,5 µl RNasin Promega, 1 µl RT Promega (MMLV), 2 µl H₂O)

Reaction is performed for 1h at 37°C and RT is inactivated by 10 min at 70°C on a BIORAD T100 thermal cycler.

cDNAs are diluted 1:10, aliquote by 10µl and stored at -20°C

As we design our primers to span different exons, we do not use « no RT » control for each sample.

qPCR :

Triplicates are always better than duplicates, but more expensive. As qPCR is very reproducible in our hands we use duplicates. Should the CV of a sample >4%, this sample is discarded and should be analyzed again . It is however much more important to have biological repeats.

cDNA are diluted 1 :10 and 2µl is used for each qPCR. Add 8µl of the reaction mix (5µl of 2X syber IQ supermix (Biorad), 330nM final concentration of each Forward and Reverse primers).

For each gene tested we use one “no template” control (no cDNA in QPCR) to check for contaminants in mixes and that is important for the melting curve (detection of primer dimers). Primers have been verified for efficiency on a comparable sample (same tissue, cell type...) → see primer design.

We use HPRT as our reference gene that display a similar abundance to our genes of interest (usually HPRT for Cq around 24).

Samples are run on a BioRad CFX96 qPCR machin. The program used is universal, and the same for all the primers. The program end with a « melting curve » step to verify that only one amplicon is produced with neither water contamination nor primer dimers.

Program : 95°C 3'essential for release of the Taq chemical inhibition, (95°C 10" denaturation, 64°C 30" annealing / elongation, plate read out) x40, from 65 to 95°C, 5" every 0,5°C, read-out to determine the melting curve.

Primer design and validation :

We use primer blast (primer3 + blast) on http://www.ncbi.nlm.nih.gov/tools/primer-blast/index.cgi?LINK_LOC=BlastHome. The most important criteria are :

-primers must span an exon-exon junction” or “Primer pair must be separated by at least one intron on the corresponding genomic DNA” (to avoid amplification of contaminating genomic DNA).

-Amplified fragment should be between 80bp and 150bp. Tm around 60-62-64°C.

-%GC between 40% and 60%.

To test the efficiency of each primer pair, we performed a standard curve on cDNA dilutions spanning at least 4 or 5 log, and also a negative control. cDNA should be from the same tissue as our samples. Efficiency is calculated, by the following formula : $Eff = 10^{-1/slope} - 1$. It should be as close as possible to 100%, we qualify primers between 90 and 110% ($3.6 > slope > 3.1$) This experiment also checks for the unicity and size of the amplicon and the absence of primer dimerization.

Data analysis.

We are using the Software provided with the CFX, id BioRad CFX Maestro, use CFX Manager. Cq is automatically determined by the software. We consider a Cq of 35 as the upper limit of sensitivity. Melting curve is provided for each sample, and amplification efficiency can be measured.

The $2^{-\Delta\Delta Cq}$ method is used for standardization using HPRT as the reference gene and control group was CHOW fed, HFD fed or PTU CTRL groups. We verify duplicate reproducibility and use the average value. Statistics (average, standard deviation, etc...) are made with biological repeats, not technical repetitions. The numbers of mice used for each experiment are reported in each figure legend, but never lower than 5.

Supplemental information titles and legends

Fig. S1: *CRE activity in the peripheral metabolic organs*

$Cre3^{(Tg/+)}RosatdTomato^+$ and $RosatdTomato^+$ mice (n=3 per genotype), were dissected and their tissues observed under the Leica M205FA fluorescent stereomicroscope. The green line delimits the $Cre3^{(Tg/+)}RosatdTomato^+$ (upper) from the $RosatdTomato^+$ (lower) organs. Results are shown from one mouse of each genotype that is representative of the 3.

Fig. S2: *Neuron-specific Cre-mediated recombination in different hypothalamic nuclei in mice bearing the Cre3 transgene ($Cre3^{(Tg/+)}RosatdTomato^+$ mice).*

All cells expressing tdTomato (reporter for Cre recombination) also expressed NeuN (neuronal marker), whereas none of them expressed GFAP (glial cell marker). In the rostral hypothalamus, at the level of the (A) paraventricular nucleus of the hypothalamus, about 20% of NeuN+ cells also expressed tdTomato. At the level of the (B) rostral ventromedial hypothalamus, about 40% of NeuN+ cells also expressed tdTomato. At the level of the (C) caudal ventromedial hypothalamus, about 20% of NeuN+

cells also expressed tdTomato. For each brain level, the red squares in DAPI images help locate the fields shown with higher magnification for tdTomato, NeuN and GFAP labellings. Arrows have been added to help checking that all tdTomato+ cells were also NeuN+.

Fig. S3: Characterization of the NTRKO mice: a model of selective blockade of T3 signaling in neurons.

(A) Concentration of free T3 and free T4 were measured in the plasma of the different groups of mice used in the study. The white and black marks/columns, respectively, represent CTRL and NTRKO. (B) 3- to 4-month old males from NTRKO and CTRL rendered hypothyroid by propyl-thio-uracil (PTU) and treated (n=6 per genotype) or not by T3/T4 (TH) (n=6 per genotype) were sacrificed and BAT, iWAT, Heart (He) and Liver (Li) sampled for RNA preparation. Expression of well characterized T3 target genes measured in BAT, iWAT, Heart (He) (*Klf9* and *Hr*) and Liver (Li) (*Klf9* and *Spot14*) was analyzed by relative RT-qPCR. CTRL PTU, NTRKO PTU, CTRL PTUTH, and NTRKO PTUTH are, respectively, represented by white, black, light gray, and dark gray bars. (C) Concentration of total cholesterol and triglycerides were measured in the plasma of the different groups of mice used in the study (Chow same groups as in Figure 3, HFD same groups as in Figure 5. White and Black marks/columns respectively represent CTRL and NTRKO. Ns stands as non-significant.

Fig. S4: T3 signaling in neurons regulates EE but the expression of BAT thermogenesis and I WAT browning are not altered in CHOW fed NTRKO.

6-month-old male mice CTRL and NTRKO fed a CHOW diet (n=5 and n=7) at 23°C were also sacrificed to sample BAT and iWAT for relative RT-qPCR analyzes. Markers of adrenergic response/BAT activity in (A) BAT and browning in the (B) iWAT were analyzed by relative RT-qPCR. The white and black columns, respectively, represent CTRL and NTRKO. Significance was calculated for CTRL/NTRKO. ns stands for non-significant.

Fig. S5: *Blocking T3 signaling in neurons does not affect cold-induced thermogenesis*

Five 4-month-old CTRL (n=6) and NTRKO (n=6) male mice were housed at 4°C for 58 h. (A) BAT activation was evaluated daily by thermography, average values were calculated from the data obtained for all mice before and after 24h or 48h at 4°C. (B) iWAT were sampled after cold-exposure for histology and RT-qPCR analyzes. (left panel) UCP1 immunostaining was performed on iWAT slices and quantified by image analysis. (right panel) Browning markers in iWAT were analyzed by relative RT-qPCR. White and black squares/columns respectively represent CTRL and NTRKO. Significance was calculated for a given organ between the two temperatures in A and between CTRL/NTRKO in B. ns stands for non-significant.

Fig.S6: *Blocking T3 signaling in neurons did not modify the expression of thermogenic markers, neither in BAT nor in skeletal muscle under an HFD.*

BAT and Skeletal muscles were sampled from 6-month-old male mice either CTRL or NTRKO fed a HFD for 3 months (n=5 and n=7). (A) BAT was used for histology or RNA preparation. (left panel) UCP1 immunostaining was performed and quantified on BAT slices. (right panel) The expression of *thermogenic markers* in BAT were assessed by relative RT-qPCR. Skeletal muscles were used for RNA preparation. (B) Expression of *thermogenic markers* in muscles were assessed by relative RT-qPCR. The white and black columns, respectively, represent CTRL and NTRKO. CTRL animals were taken as the reference group. Significance was calculated for CTRL/NTRKO. ns stands for non-significant.

Figure. S7: *Blocking T3 signaling in neurons in NTRKO mice did not alter their response to Diet Induced Obesity (DIO) at 30°C*

3-month-old male mice either CTRL (n=6) or NTRKO (n=5) were housed at 30°C fed a CHOW diet and then switched to a HFD (D0). (A) Body weight gain (Δ body weight) was calculated between any time point and the day diet was switched to HFD. UCP1 immunostaining was performed and quantified in

(left panel) BAT and (right panel) iWAT isolated from CHOW-fed male mice housed at 30°C. The white and black columns, respectively, represent CTRL and NTRKO. Significance was calculated for CTRL / NTRKO. ns stands for non-significant.

Fig. S1: color

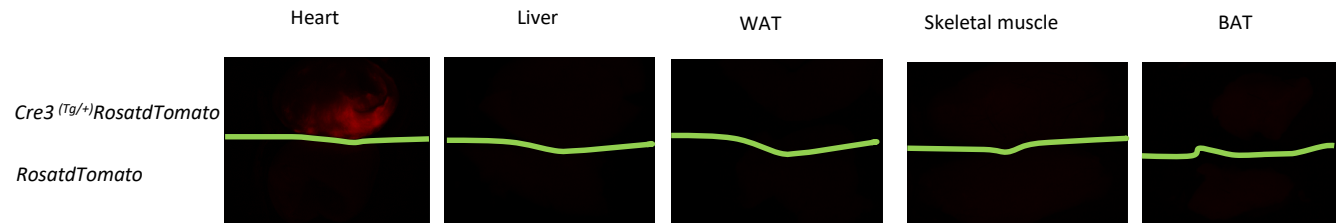


Fig. S2: color

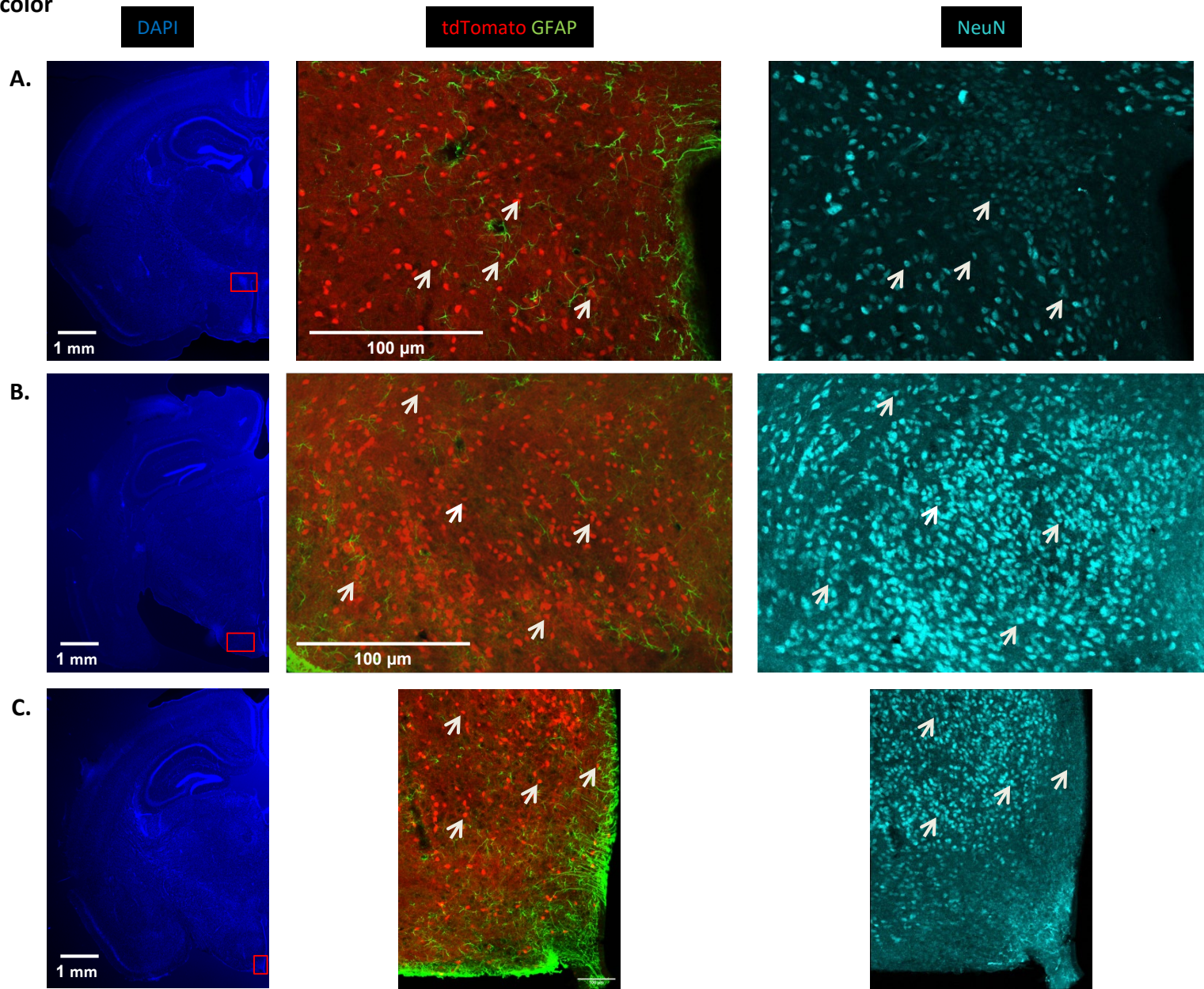


Fig. S3:

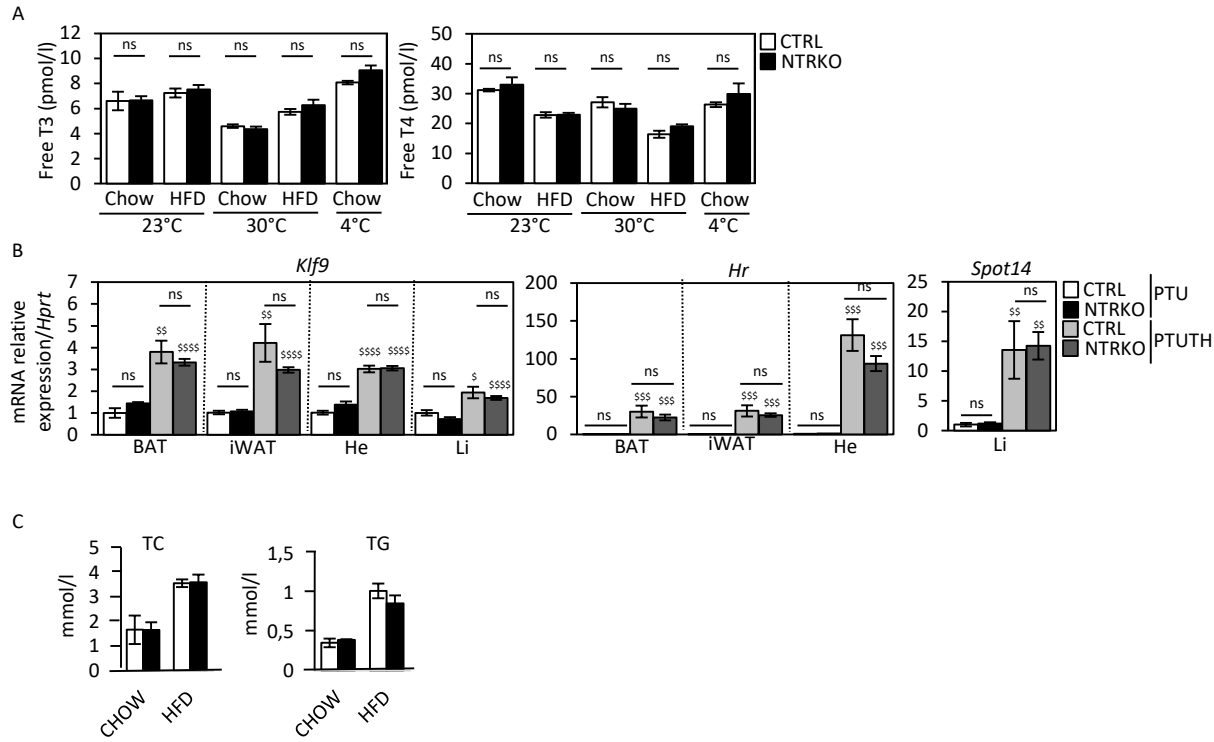


Fig. S4:

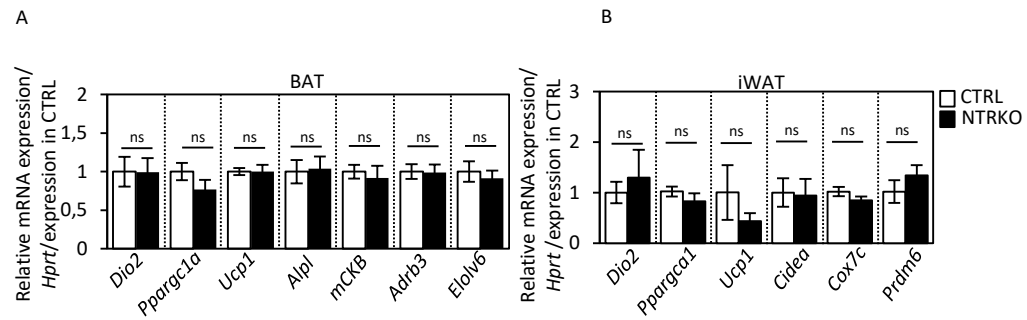


Fig. S5:

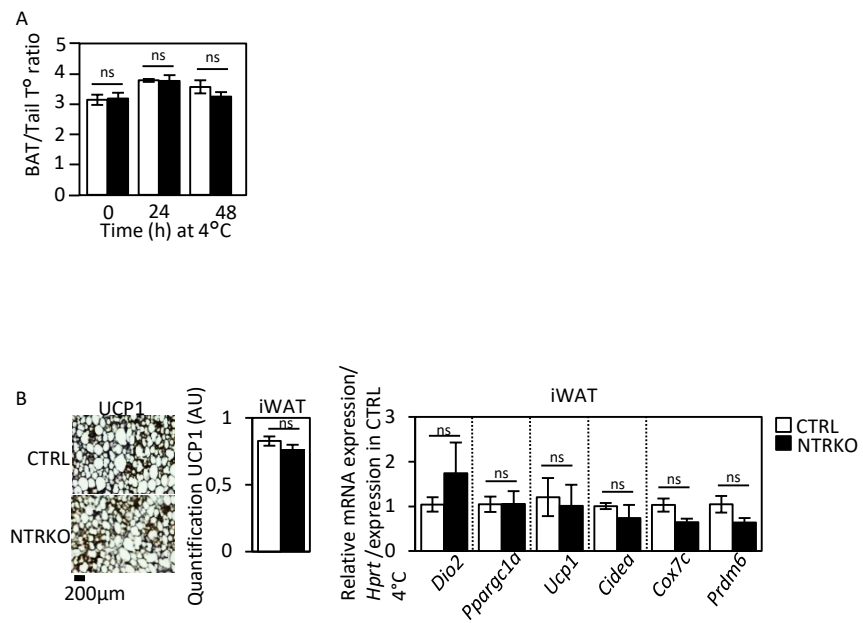


Fig. S6:

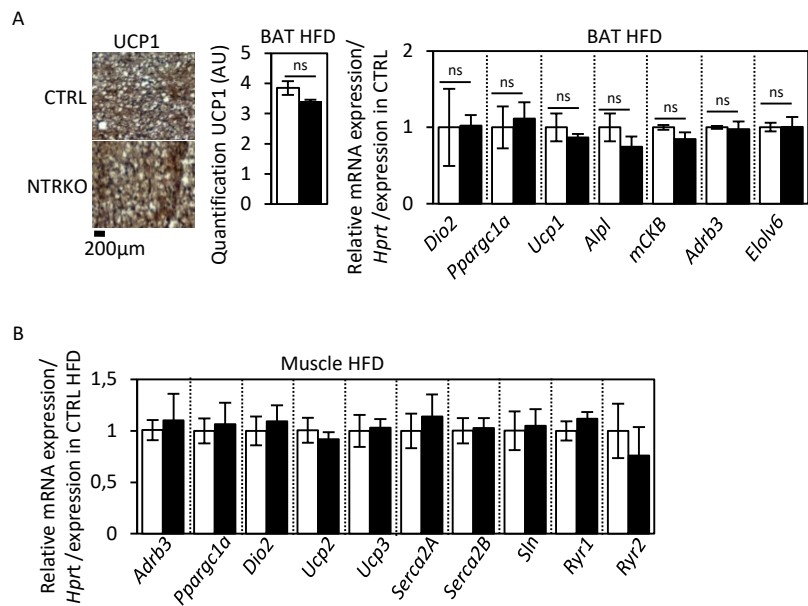


Fig. S7:

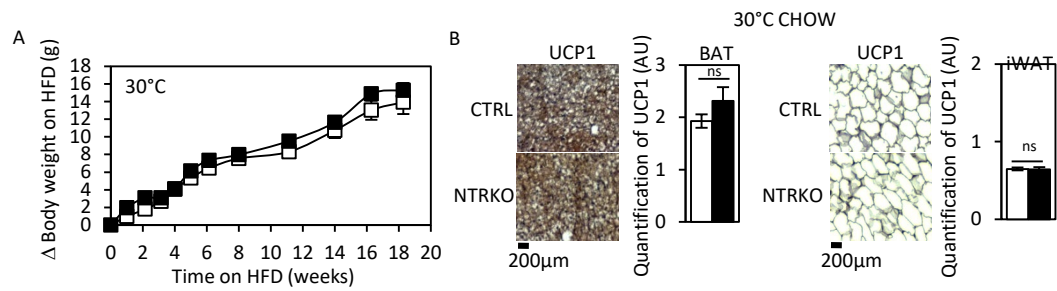


Table S1

	Forward primer	Reverse primer
Adrb3	TCC TTC TAC CTT CCC CTC CTT	CGG CTT AGC CAC AAC GAA CAC
Alpl	CCGGGGACATGCAGTATGAATTG	TGGTCAATCCTGCCTCCTCC
Cidea	TGACATTCATGGGATTGCAGAC	GGCCAGTTGTGATGACTAAGAC
Cox7c	CCA GAG TAT CCG GAG GTT CA	GAA AGG TGC GGC AAA CC
Dio2	CCT AGA TGC CTA CAA ACA GGT TAA A	TGT TAC CTG ATT CAG GAT TGG A
Elovl6	ACAATGGACCTGTCTAGCAAA	GTA CCA GTG CAG GAA GAT CAG T
Hprt	CAGCGTCGTGATTAGCGATG	CGAGCAAGTCTTTCAGTCCTGTCC
Hr	AGAGGTCCAAGGAGCATCAAGG	GCCTTGCTTCTATGATTGTCTCC
Klf9	CACGCCTCCGAAAAGAGGCACAA	CTTTTCCCAGTGTGGGTCCGGTA
mCBK	TGACCTGGACCCCAACTACG	AGGCTGGACAGAGCTTCTACTG
Ppargc1a	GAT GGC ACG CAG CCC TAT	CTC GAC ACG GAG TTA AAG GAA
Prdm6	CCCACATTCCGCTGTGAT	CTCGCAATCCTTGCACTCA
Ryr1	GAGTCTAAGCGCCAGTTCATCTTC	GCTCACGAACAGCTCCATCTTC
Ryr2	ATGGCTTTAAGGCACAGCG	CAGAGCCCGAATCATCCAGC
Serca2a	GTCATTTTCCAGATCACACCG	GTTACTCCAGTATTGCGGGTTG
Serca2b	ACCTTTGCCGCTCATTTTCCAG	AGGCTGCACACACTCTTTACC
Shh	AGCAGGTTTCGACTGGGTCTAC	ATTTGGCCGCCACGGAGTTC
Sln	GTCCTCTTCAGGAAGTGAAG	TGGCCCCTCAGTATTGGTAGG
Spot14	CTC GGA GGA GCT GGA CCT A	GTG ATG GAG GCT GCA GAA GT
Thrb	AGCCAGAACCACGGATGAGGA	TGCCACCTTCTGGGGCATTAC
TRH	CTTGGTGCTGCCTTAGATTCCTG	CCAGGGTGCTGCTGTTTGTG
Ucp1	AAG CTG TGC GAT GTC CAT GT	AAG CCA CAAA CCC TTT GAA AA
Ucp2	GCCTCTGGAAGGGGAGTTCTC	ACCAGCTCAGCACAGTTGACA
Ucp3	TTTCTGCGTCTGGGAGCTT	GGCCCTCTTCAGTTGCTCAT